

Threshold Functions, Node Isolation, and Emergent Lacunae in Sensor Networks

Srisankar S. Kunniyur and Santosh S. Venkatesh[†]

Abstract

Battery lifetimes in wireless sensor networks are dictated by usage patterns and the elected transmission power. As batteries fail there is an inevitable devolution of the network characterised by the emergence of isolated nodes, the growth of sensory lacunae or dead spots in the sensor field and, eventually, a breakdown in connectivity between the surviving nodes of the network. A Euclidean random graph model with node extinctions governed by an arbitrary lifetime distribution is introduced to explicate fundamental features of these phenomena. Sharp limit theorems characterising the time at which these phenomena make their appearance are derived and, in particular, threshold functions (or phase transitions) are shown for the time at which isolated nodes, discs, and, more generally, lacunae appear. It is shown that at the critical times the number of emergent lacunae follow an asymptotic Poisson law for any distribution of battery lifetimes (though the location of the threshold depends on the particular distribution). These results provide explicit and fundamental tradeoffs between transmission power, vertex density, field coverage, and network lifetime and suggest how principled choices may be made.

1 Introduction

Recent advances in sensor technology, low-power RF design and portable computing have enabled the development of densely distributed, wireless micro-sensor networks (cf. Chandrakasan, *et al* [2], Clare, *et al* [3], and Dong, *et al* [4]). Applications of such sensor networks include their deployment in battlefields, disaster stricken areas, environment monitoring systems and space exploration. A main feature of such networks is the untethered nature of the sensors a consequence of which is that the battery power at each sensor becomes the primary resource constraint. These networks hence exhibit a particularly transient nature with ongoing vertex failures due to battery exhaustion causing a continual devolution of the network with a concomitant degradation of functionality. The projected “lifetime” of these networks hence plays an important role in their deployment.

Previous work on dense sensor networks has concentrated on the critical power required for asymptotic connectivity. In this context, the most comprehensive and precise results are provided by Penrose [16] in a general random geometric graph setting; Gupta and Kumar [8] and Xue and Kumar [20] provide detailed related analyses in the sensor

Key words and phrases. Sensor networks, graph connectivity, random graphs, threshold functions, phase transitions, Poisson paradigm, inclusion-exclusion.

[†]Corresponding author.

A short version of this paper was presented at WiOpt’04, Cambridge, March 2004 [12]. This version of the paper was printed on September 1, 2004.

network context. These investigations assume a dense uniform distribution of the vertices to answer the fundamental question: What is the communication radius (or number of neighbours) required at each sensor to ensure initial network connectivity? Similar questions are considered by Shakkottai, *et al* [17] when a certain fraction of vertices placed on a grid are functional at any given time. These results are concerned with establishing initial connectivity or coverage. There is much less known, however, about how such a network devolves as vertices degrade and fail over time, primarily due to limited battery power at the vertices.

Battery lifetimes in wireless sensor networks are dictated by usage patterns and the transmission power at each vertex. As batteries fail there is an inevitable devolution of the network characterised by the growth of sensory lacunae or dead spots in the sensor field and eventually a breakdown in connectivity between the surviving vertices of the network. We investigate fundamental attributes of these phenomena in a simple model of randomly deployed sensors where the battery lifetimes of the sensors are independent random variables with a common but arbitrary lifetime distribution parametrised by the power expenditure and the mean usage. In this somewhat sanitised but fundamental setting we derive sharp limit theorems characterising the time at which these phenomena make their appearance. A characteristic feature is the appearance of *phase transitions* or *threshold functions*: emergent (disruptive!) phenomena appear abruptly in a sharply concentrated time span. Our results provide explicit tradeoffs between transmission power, vertex density, and the time to emergence of various phenomena and suggest how efficient choices may be made, while providing partial answers to the following fundamental questions:

- *When does the network fail?*
- *What is the distribution of failures in the network?*

The included examples illustrate the tradeoffs in various cases.

On notation: All logarithms are to base e , \mathbf{P} stands for probability measure in the underlying probability space, and \mathbf{E} stands for expectation. Points in the Euclidean plane are denoted x , x_i , etc. For any point $x = (x_1, x_2)$ in the plane, $|x| = \sqrt{x_1^2 + x_2^2}$ denotes the Euclidean norm of x .

We will use the following variants of the Landau notation. Suppose $\{f_n\}$ and $\{g_n\}$ are real sequences. As $n \rightarrow \infty$ we say that $f_n = \mathcal{O}(g_n)$ if $|f_n| \leq K|g_n|$ for some positive constant K , and $f_n = \mathfrak{o}(g_n)$ if $|f_n|/|g_n| \rightarrow 0$, and $f_n \sim g_n$ if $f_n/g_n \rightarrow 1$. Note that the “big-O” and “small-o” variants in use here refer to absolute values. In consequence we will occasionally encounter an expression of the form $1 + \mathfrak{o}(1)$ for a probability—the context makes it clear that the small-o order term must in fact be a negative, asymptotically vanishing quantity. The order terms we encounter will all be ultimately negligible and their signs will not matter. We will also commit the mild notational solecism of stringing together order relations: an expression of the form $f_n = \mathcal{O}(g_n) = \mathfrak{o}(h_n)$ means (a) that $f_n = \mathcal{O}(g_n)$ and (b) that $g_n = \mathfrak{o}(h_n)$. Of course, this also implies that $f_n = \mathfrak{o}(h_n)$ and we compact this syllogism into a single equation in the hope that there is no danger of confusion as to what is meant.

2 Hard-Sphere Models, Deployment, and Extinction

In this section we describe a sanitised setting in which a multihop network of functionally equivalent sensors is deployed to detect and report phenomena that may occur uniformly across a target region. Our focus will be on the graph-theoretic properties of connectivity and coverage—and their devolution in time as vertices fail—and we eschew considerations

of network-specific details such as the locations of sinks and collector nodes. This setting provides perhaps the cleanest venue in which the fundamental results can be seen without obfuscation. We will defer a brief discussion of the limitations of the model and perhaps more realistic extensions to Section 6.

A Hard-Sphere Models of Communication and Sensing

We consider a sensor field comprised of a circle of unit radius in which n sensors are to be dispersed. Sensors are assumed to be dimensionless nodes equipped with both a sensing and a communication capability. We will suppose that each sensor can sense events within a distance s from it and can communicate with any other sensor located within a distance c from it. This is the so-called “hard-sphere” model of sensing and communication.

The power expended by a sensor during transmission is monotonically related to the communication radius, typically via a power law. As the available sensor power is the critical scarce resource in this setting, in order to conserve power one can imagine a deployment where sensors utilise their neighbours to relay information through the network in a series of small hops. We will not be concerned with protocol issues here, though these can be thorny, but instead focus on how transmission power requirements may be reduced by increasing the density of sensors on the ground. Accordingly we will suppose that the communication radius $c = c_n$ is a suitably decaying function of the number of sensors n . The key requirement in this context is that the communication radius be chosen large enough to ensure connectivity.¹

Unlike transmission which is an active operation initiated by a sensor, in this context we view sensing as a largely passive operation. Sensing at larger and larger distances would imply detection of phenomena at weaker and weaker signal-to-noise ratios which would presumably require the implementation of more sophisticated algorithms on chip resulting in a higher power consumption. This may be taken as a justification of a hard-sphere model for sensing as well, at least as an initial attempt at modelling the situation, with the sensing radius $s = s_n$ of each sensor also some decaying function of n .

A variety of questions may be posed about coverage, at various levels of formality. For instance, for a given deployment model, one may be interested in how many sensors will need to be deployed to completely cover the sensor field. Alternatively, for a given number of sensors, one may be interested in the area of the sensor-blind region, or, yet again, in the area of the largest contiguous region that is left uncovered. Of course, many such similar questions can be posed. Coverage issues such as these have a distinguished history and have received substantial attention in the literature (cf. Hall [9] and Meester and Roy [15] for two relatively recent compendia).

Our focus in this paper is on coverage in the following limited sense. We begin with a connected network, the density of sensors on the ground assumed sufficient for the coverage needs at hand. As sensors fail over time we then track the appearance of lacunae or sensory dead spots *within* the originally established network; the appearance of lacunae of a given size is a quantitative measure of how coverage within the network degrades over time. Our main result in this context is the demonstration of a sharp Poisson law for the first appearance of isolated nodes and lacunae. In particular, the result implies a phase transition or threshold function for coverage failure within the network.

¹In practice, a variety of algorithms may be deployed to adaptively operate each sensor node at the minimum requisite power needed to communicate with its neighbours (cf. Kawadia *et al.* [11], Wattenhofer *et al.* [19] and Cerpa and Estrin [1] and the references therein for recent results.)

B Deployment, Initial Connectivity and Coverage

We suppose that the sensors are deployed randomly with locations X_1, \dots, X_n assumed to be drawn independently from the uniform distribution in the unit circle. If each sensor is assumed capable of communicating with other sensors within a distance $c = c_n$ of it then the sensor locations determine a (random) communication network whose links are all short hops of length no more than c . A fundamental property of interest in this setting is whether the network is connected, at least initially, immediately after deployment.

As may be anticipated, the network will be almost surely connected (for large n) if the communication radius c_n is sufficiently large. A known result asserts indeed that $\sqrt{(\log n)/n}$ is a threshold function for the radius at which network connectivity appears abruptly (cf. Penrose [16] for rather more precise and general results in a graph-theoretic setting; Gupta and Kumar [8] provide an analysis in the current framework; for a modest tightening of the results and extensions see Venkatesh [18]; the classical result is due to Erdős and Renyi [5]).

We will take for granted that communication connectivity is a sine qua non in this framework and accordingly will be concerned mainly with the situation when the network of sensors is initially connected. The communication radius $c = c_n$ will hence have to be at least of the order of $\sqrt{(\log n)/n}$.

The coverage of the sensing field that is achieved depends on the sensing radius $s = s_n$. It is known that the critical sensing radius to achieve complete coverage of the unit circle is again $\sqrt{(\log n)/n}$ to first order though the asymptotic rate is slightly larger than that for c_n (cf. Hall [9]). If s_n is comparable to r_n at the critical communication radius ensuring connectivity, for instance, most of the area of the field will be within the region of coverage of at least one sensor though there may be small gaps in coverage. If $s_n = 0$, on the other hand, we have a point sensing model where coverage in the connected network is only at the sensor locations. We make no assumptions about the choice of the sensing radius s_n but suppose that it is selected with an eye to the coverage needs at hand.

C Node Extinctions

Each sensor is equipped with a battery which has a finite lifetime determined by the usage patterns of the sensor and the selected communication radius. Let T_1, \dots, T_n denote the random lifetimes of the batteries of the n sensors. We will suppose that these lifetimes are independent random variables with a common distribution $\mathbf{P}\{T_i \leq t\} = F(t) = F_c(t)$. It will be convenient to also introduce the notation $1 - F(t) = G(t) = G_c(t)$ for the probability that the battery lifetime exceeds t . As indicated in the notation, the lifetime distribution is considered to be parametrised by the communication radius supported by the battery; larger choices of c permit a smaller deployment of vertices while guaranteeing connectivity, but also deplete individual batteries faster; smaller choices of c will deplete batteries slower but require a larger numbers of sensor nodes to maintain connectivity, with a concomitant increase in the likelihood of node extinctions by a given time. While we make no further assumptions about the nature of the lifetime distribution G_c , for a given level of deployment, and abeyant sophisticated routing, communication over larger ranges may be expected to consume more power. Natural parametrisations may hence be expected to exhibit uniform majorizations of the form $G_{c_1} \geq G_{c_2}$ whenever $c_1 < c_2$.

The parametrisation of lifetime by communication radius takes account of the fact that communication typically consumes more power than computation or sensing. While this is the main parametrisation that we will consider in this paper, the notation, analysis, and results segue over smoothly to the situation where the lifetime distribution is parametrised

additionally by the choice of sensing radius s with $G = G_{c,s}$. Further parametrisations by, say, a random, node-dependent usage-parameter α_i are also possible, $G = G_{c,s,\alpha_i}$. The framework easily handles cases where the α_i s are independent and drawn from a common distribution. Dependencies across node usages are, however, much harder to handle and while it is likely that our main results will continue to hold under mild dependencies, significant caveats on the dependency structure will have to be spelled out.

3 Poisson Laws for Isolated Vertices, Discs, and Lacunae

For each $r > 0$, the sensor locations induce a *random geometric graph* $\mathcal{G}_{n,r} = \mathcal{G}_{n,r}(X_1, \dots, X_n)$ whose vertices are the points X_1, \dots, X_n in the plane. A pair of vertices (X_i, X_j) forms an edge of the graph if, and only if, $|X_i - X_j| \leq r$. If (X_i, X_j) is an edge of the graph we say that the vertices X_i and X_j are *adjacent*. The graph $\mathcal{G}_{n,r}$ hence has an intrinsically geometric character and we will refer to the X_i as vertices or points depending on whether we wish to emphasise the graph or geometric attribute. Connectivity and coverage questions may be posed in terms of the graph $\mathcal{G}_{n,r}$ for suitable choices of $r = r_n$.

A Isolated Vertices and Discs

As time passes and sensor nodes are extinguished the ability of the network to sense and report sensory phenomena at and in the vicinity of the nodes gets compromised. Say that a vertex X_i is *live at time* t if $T_i > t$. We also say that sensor node i is live to mean the same thing.

DEFINITION 1 A vertex X_i of the graph $\mathcal{G}_{n,r}$ is *isolated at time* t if there are no live vertices X_j adjacent to X_i at time t in $\mathcal{G}_{n,r}$.²

In other words, vertex X_i in $\mathcal{G}_{n,r}$ is isolated at time t if $T_j \leq t$ for every vertex X_j adjacent to X_i in $\mathcal{G}_{n,r}$. If a vertex is isolated in $\mathcal{G}_{n,c}$ then phenomena detected by the node at that location cannot be communicated to the rest of the network; likewise, if a vertex is isolated in $\mathcal{G}_{n,s}$ then no node in the network at large can sense phenomena at that node's location. Thus, if vertex X_i is isolated in $\mathcal{G}_{n,\max\{c,s\}}$ at time t then the network at large would thereafter be sensorily blind to phenomena at the location of node i . The conclusion is slightly conservative as it ignores the condition of node i itself and we will refine this picture of sensory isolation a little; but first, a generalisation expanding the idea of geometric isolation from a point to a disc.

For $\ell \geq 0$, write $\mathbb{D}(\ell; x) = \{y : |y - x| \leq \ell\}$ for the Euclidean disk of radius ℓ centred at x and, in a slight abuse of notation, for any $0 \leq \ell_1 < \ell_2$, write $\mathbb{D}(\ell_1, \ell_2; x) = \mathbb{D}(\ell_2; x) \setminus \mathbb{D}(\ell_1; x) = \{y : \ell_1 < |y - x| \leq \ell_2\}$ for the annulus between the discs of radius ℓ_1 and ℓ_2 centred at x . To keep notation unburdened we will write $\mathbb{D}_i(\ell) = \mathbb{D}(\ell; X_i)$ for the disc of radius ℓ centred at vertex X_i and, likewise, $\mathbb{D}_i(\ell_1, \ell_2) = \mathbb{D}(\ell_1, \ell_2; X_i)$ for annuli centred at vertex X_i .

DEFINITION 2 The disc $\mathbb{D}_i(\ell)$ is *isolated at time* t in $\mathcal{G}_{n,r}$ if the annulus $\mathbb{D}_i(\ell, \ell + r)$ contains no live vertices at time t .

²It should be noted that the definition of isolation adopted here is subtly different from the more usual graph-theoretic notion of isolated vertices. In our context, when a vertex is extinguished all edges incident on it are removed but the vertex itself is not. The major part of the motivation is *geometric*: we will be able to extend the notion to isolated geometric *regions* centred at vertices which may or may not be live. As a minor note, our definition allows of the possibility that passive sensing may continue at a node well after active communication capability has eroded.

The case $\ell = 0$ returns us to the notion of an isolated vertex. Lacunae or sensory dead spots at and in the vicinity of network nodes emerge with the appearance of isolated discs centred at node locations: arguing as before, if $\mathbb{D}_i(\ell)$ is isolated at time t in $\mathcal{G}_{n, \max\{c, s\}}$ then the network at large will be unable to register phenomena originating subsequently in the disc of radius ℓ centred at the location of node i .

We are interested in what can be said about the distribution of the number of isolated vertices and discs of a given size, and their evolution in time for a given lifetime distribution $G(t) = G_c(t) = \mathbf{P}\{T_i > t\}$. Write ${}^\ell N(t; r, c)$ for the number of isolated discs of radius ℓ centred at network vertices at time t in the graph $\mathcal{G}_{n, r}$. In particular, ${}^0 N(t; r, c)$ is the number of isolated vertices at time t in $\mathcal{G}_{n, r}$. Our main result asserts a sharp limit theorem for ${}^\ell N(t; r, c)$ in a suitable range.

MAIN THEOREM *Let λ be any fixed positive constant. Suppose ℓ_n, r_n, c_n , and t_n are non-negative sequences and let $R_n = \sqrt{2\ell_n r_n + r_n^2}$. Suppose these sequences satisfy the asymptotic properties*

$$R_n = o\left(\frac{\log n}{\sqrt{n}}\right) \quad \text{and} \quad R_n^2 G_{c_n}(t_n) = \frac{1}{n} \log \frac{n}{\lambda} + o\left(\frac{1}{n}\right) \quad (1)$$

as $n \rightarrow \infty$. Then ${}^{\ell_n} N(t_n; r_n, c_n)$ converges in distribution to the Poisson distribution with mean λ . More specifically, for every fixed non-negative integer m , $\mathbf{P}\{{}^{\ell_n} N(t_n; r_n, c_n) = m\} \rightarrow e^{-\lambda} \lambda^m / m!$ as $n \rightarrow \infty$.

For the specific case of isolated vertices in the communication graph $\mathcal{G}_{n, c}$ we obtain the following useful specialisation.

COROLLARY 1 *Suppose the sequences c_n and t_n vary with n such that*

$$c_n = o\left(\frac{\log n}{\sqrt{n}}\right) \quad \text{and} \quad c_n^2 G_{c_n}(t_n) = \frac{1}{n} \log \frac{n}{\lambda} + o\left(\frac{1}{n}\right) \quad (1')$$

as $n \rightarrow \infty$. Then the number of isolated vertices at time t_n in the graph \mathcal{G}_{n, c_n} converges in distribution to the Poisson distribution with mean λ and a fortiori the probability that there are no isolated vertices in the graph \mathcal{G}_{n, c_n} tends to $e^{-\lambda}$.

REMARKS: A few remarks are in order before we proceed to examples and proofs.

1. The choice of the disc of unit radius as the sensor field saves a little in the notation. If the sensor field is a disc of radius M we only need to replace the second equation in (1) by $R_n^2 G_{c_n}(t_n) = \frac{M^2}{n} \log \frac{n}{\lambda} + o\left(\frac{1}{n}\right)$. As will be apparent from the proof, matters don't change materially for a general sensor field. If the field is geometrically nice and has area \mathfrak{A} , the theorem will hold with the second equation in (1) replaced by $R_n^2 G_{c_n}(t_n) = \frac{\mathfrak{A}}{\pi n} \log \frac{n}{\lambda} + o\left(\frac{1}{n}\right)$. Here "niceness" means roughly that the perimeter of the field is not dominant vis à vis the interior.
2. The dependence of ${}^{\ell_n} N(t_n; r_n, c_n)$ on c_n is implicit through the parameterisation of the lifetime distribution $G(t) = G_{c_n}(t)$ by the communication radius c_n . As will become clear in the examples below, this parametrisation is both natural and critical.
3. The conditions embodied in (1') restrict c_n to asymptotic orders between $\sqrt{(\log n)/n}$ and $(\log n)/\sqrt{n}$ (as $G_c(t)$ is majorized by 1 for all c). The order of the lower bound cannot be improved as a radius of order at least $\sqrt{(\log n)/n}$ is requisite for connectivity in the communication graph, as remarked earlier; in particular, the connectivity

region is solidly within the province of the theorem. As we shall see in the course of the proof, the upper bound for the rate for c_n embodied in the latter condition also turns out to be best possible for the stated results to hold; more generally, *the rates embodied in (1) are essentially best possible.*

Under the conditions of the theorem, the probability that there are no isolated discs tends to $e^{-\lambda}$ whence the probability that there are one or more isolated discs tends to $1 - e^{-\lambda}$. The choice of the positive λ will determine which of the two situations is likely to prevail: a small λ makes it unlikely that any discs are isolated in the time frame of interest while a large λ makes it rather likely that discs will become isolated. For a given parametric family of distributions $G(t) = G_{c_n}(t)$, the conditions (1,1') determines the critical value of time $t = t_n$ at which there is a threshold function (or *phase transition*) and isolated discs (vertices) begin to appear. Some illustrative examples for the case of isolated vertices ($\ell_n = 0$) in the communication graph \mathcal{G}_{n,c_n} may help flesh out the asymptotics.

EXAMPLE 1 *Exponential decay, high drain.* Consider a random deployment of sensors in a circular sensor field of radius M . In this case the second condition in (1') is replaced by (see the remarks following the main theorem)

$$G_{c_n}(t_n) = \frac{M^2}{nc_n^2} \log \frac{n}{\lambda} + o\left(\frac{1}{nc_n^2}\right).$$

We may model increased drain on a battery due to larger communication radii via a power law in c_n . A fourth-power law in c_n would connote, for example, adverse conditions and a high-drain situation. If we now consider a memoryless distribution for the battery lifetimes, we obtain a distribution of the form $\mathbf{P}\{T_i > t\} = G_{c_n}(t) = e^{-\alpha c_n^4 t}$ where α may represent a mean usage parameter. Routine calculations now show that the critical range for t is

$$t_n = \frac{1}{\alpha c_n^4} \left[\log(nc_n^2) - \log \log n - 2 \log M + \frac{\log \lambda}{\log n} + o\left(\frac{1}{\log n}\right) \right].$$

For example, if the communication radius is at the critical range required for connectivity, say, $c_n = M \sqrt{\frac{\log n + \kappa}{n}}$ for a suitably large positive κ , then $t_n \sim n^2 \log(\lambda e^\kappa) / \alpha M^4 \log^3 n$ so that the critical range of time at which isolated vertices begin to appear for the first time is of the order of $n^2 / \log^3 n$. If the communication radius is super-critical, however, a similar analysis shows that isolated vertices crop up somewhat earlier in time. If, for instance, $c_n = \sqrt{\log^2(n) / n \log \log n}$ then the critical range of time is asymptotic to $n^2 (\log \log n)^3 / \alpha \log^4 n$ which is $o\left(\frac{n^2}{\log^3 n}\right)$. Thus, a super-critical communication radius results in an earlier appearance of isolated vertices in accordance with naïve expectation though the explicit threshold function for the time to emergence of isolated vertices quantifies the rôle of the battery power. The next example illustrates however that quite the reverse can occur. ■

EXAMPLE 2 *Exponential decay, low drain.* With a memoryless distribution for battery lifetimes, as above, suppose now that the lifetime dependence on power varies quadratically as would be the case in a "clean" environment. In this case the lifetime distribution is of the form $G_{c_n}(t) = e^{-\alpha c_n^2 t}$ so that the critical range for t is now

$$t_n = \frac{1}{\alpha c_n^2} \left[\log(nc_n^2) - \log \log n - 2 \log M + \frac{\log \lambda}{\log n} + o\left(\frac{1}{\log n}\right) \right].$$

With initial critical connectivity $c_n = M\sqrt{\frac{\log n + \kappa}{n}}$, the threshold function for the appearance for isolated vertices is asymptotic to $t_n \sim n \log(\lambda e^\kappa) / \alpha M^2 \log^2 n$ which is of the order of $n / \log^2 n$. For super-critical initial connectivity $c_n = \sqrt{\log^2(n) / n \log \log n}$ the critical range of time is now asymptotic to $n(\log \log n)^2 / \alpha \log^2 n$ which increases faster than $n / \log^2 n$. In this model, a super-critical initial radius for connectivity ensures a longer period of time before the first appearance of isolated vertices. *Thus, while a lower density of vertices (near the critical number needed for connectivity) is preferred when the drain is high, quite the reverse is true when the drain is low.* \blacksquare

EXAMPLE 3 *Regularly varying distributions.* Karamata's [10] theory of regularly varying functions yields a large range of useful heavy-tailed distributions. For example, let $\mu(r)$ be any positive monotonically decreasing function of r . If $G_{c_n}(t) \sim \mu(c_n)t^\sigma$ as $t \rightarrow \infty$ for some $\sigma < 0$ then G is regularly varying with exponent σ . The critical range of t_n around which isolated vertices start to appear in the network is then $t_n \sim \left(\frac{M^2}{nc_n^2\mu(c_n)} \log \frac{n}{\lambda}\right)^{\frac{1}{\sigma}}$. The critical communication radius for connectivity, $c_n \sim M\sqrt{\log(n)/n}$, buys us little here unless $\mu(r)$ decreases to zero as $r \rightarrow 0$. If the communication radius is supercritical, for example $c_n \sim \sqrt{\log^2(n) / n \log \log n}$, then extinction occurs much faster at $t_n \sim \left(\frac{M^2 \log \log n}{\mu(c_n) \log n}\right)^{\frac{1}{\sigma}}$. \blacksquare

B Sensory Lacunae

As we've seen, the isolation of $\mathbb{D}_i(\ell)$ in $\mathcal{G}_{n, \max\{c, s\}}$ implies a sensory lacuna or dead spot centred at vertex X_i . A slightly more precise picture emerges if we consider the health of the sensory nodes inside the disc $\mathbb{D}_i(\ell)$ as well.

In general, the presence of a sensory dead spot of radius ℓ centred at vertex X_i implies both a cessation of sensing from without the disc *and* a cessation of communication from within the disc. More formally, there will be a sensory dead spot of radius ℓ centred at vertex X_i at time t if the following two conditions are jointly satisfied at that time:

1. No live vertex external to the disc $\mathbb{D}_i(\ell)$ has a sensory region that intersects the disc. For this condition to hold it is necessary and sufficient that there be no live vertices in the annulus $\mathbb{D}_i(\ell, \ell + s)$.
2. No live vertex within the disc $\mathbb{D}_i(\ell)$ has a communication pathway to the network at large. For this condition to hold it suffices if there are no live vertices in the disc $\mathbb{D}_i(\ell)$ or, alternatively, if there are no live vertices in the annulus $\mathbb{D}_i(\ell, \ell + c)$.

These considerations suggest the following formal characterisation of lacunae in the network.

DEFINITION 3 We say that there is a *sensory lacuna of radius ℓ centred at vertex X_i at time t* if the following two conditions are satisfied at time t : (1) the annulus $\mathbb{D}_i(\ell, \ell + s)$ contains no live vertices; and (2) at least one of the disc $\mathbb{D}_i(\ell)$ or the annulus $\mathbb{D}_i(\ell, \ell + c)$ contains no live vertices.

The latter condition is slightly conservative as it is only really requisite that there are no live vertices external to $\mathbb{D}_i(\ell)$ which are within a distance c of any live vertex in $\mathbb{D}_i(\ell)$ to make communication out of the disc $\mathbb{D}_i(\ell)$ impossible. However, at critical communication connectivity and beyond, the density of nodes on the ground is such that node separations

are no more than the order of $n^{-1/2}$; the geometrically regular picture of circles and annuli of influence that is conjured up by the definition is both analytically convenient and not far removed from the reality on the ground.

Let $u(x)$ denote the unit step function taking value 1 for $x \geq 0$ and value 0 for $x < 0$. Define

$$P_n = P_n(\ell, s, c, t) = e^{-n[(\ell + \max\{s, c\})^2 - \ell^2]G_c(t)} + (1 - G_c(t))\{e^{-n(\ell+s)^2G_c(t)} - e^{-n(\ell+c)^2G_c(t)}\}u(c-s). \quad (2)$$

We will see that if $\ell_n^2 + s_n^2 + c_n^2 = o(\frac{\log^2 n}{n})$ then the probability that there is a lacuna of radius ℓ_n at any given network vertex at time t_n is asymptotic to $P_n(\ell_n, s_n, c_n, t_n)$. As a consequence of the proof of the main theorem we then quickly obtain a Poisson law for the number of lacunae and thence a phase transition for the time to their emergence.

COROLLARY 2 *Suppose $\ell_n^2 + s_n^2 + c_n^2 = o(\frac{\log^2 n}{n})$. If $P_n(\ell_n, s_n, c_n, t_n) \sim \lambda/n$ then the number of lacunae of radius ℓ_n centred at network vertices at time t_n converges in distribution to the Poisson distribution with mean λ .*

Some examples may help to make the formidable-looking asymptotic condition intelligible.

EXAMPLE 4 $\ell_n = 0$: *point lacunae at network vertices.* Setting $\ell = 0$ in (2) yields

$$P_n = e^{-n(\max\{s, c\})^2G_c(t)} + [e^{-ns^2G_c(t)} - e^{-nc^2G_c(t)}]u(c-s) = e^{-ns^2G_c(t)}$$

for all $s \geq 0$. It follows that the number of point lacunae satisfy an asymptotic Poisson law with mean λ if $e^{-ns^2G_{c_n}(t_n)} \sim \lambda/n$. A comparison with (1,1') shows that this is equivalent asymptotically to the problem of isolated vertices in the graph \mathcal{G}_{n, s_n} . The critical time t_n at which point lacunae first emerge may now be determined as in Examples 1–3. \blacksquare

EXAMPLE 5 $\ell_n = s_n$: *lacunae over regions of nodal coverage.* With $\ell = s$ in (2) we obtain

$$P_n = \begin{cases} e^{-n[(s+c)^2 - s^2]G_c(t)} + (1 - G_c(t))\{e^{-4ns^2G_c(t)} - e^{-n(s+c)^2G_c(t)}\} & \text{if } s \leq c, \\ e^{-3ns^2G_c(t)} & \text{if } s > c. \end{cases}$$

For definiteness, now suppose $s_n = \alpha c_n$ for some $\alpha > 0$. If $0 < \alpha < 1/(\sqrt{5} - 1)$ then we are in the regime $s_n \leq c_n$ and it is easy to see that $P_n \sim (1 - G_{c_n}(t_n))e^{-4ns_n^2G_{c_n}(t_n)}$ as the other two exponential terms are sub-dominant (bear in mind that communication connectivity requirements allied with the conditions embodied in (1) will force $1 - G_{c_n}(t_n)$ to be of order at least $1/\log n$); if $\alpha = 1/(\sqrt{5} - 1)$ then $P_n \sim (2 - G_{c_n}(t_n))e^{-4ns_n^2G_{c_n}(t_n)}$; if $\alpha \geq 1$ then $P_n = e^{-3ns_n^2G_{c_n}(t_n)}$. Thus, the asymptotic expression for P_n increases smoothly from $(1 - G_{c_n}(t_n))e^{-4ns_n^2G_{c_n}(t_n)}$ to $e^{-3ns_n^2G_{c_n}(t_n)}$ as α increases. The corresponding threshold functions for t_n may be determined again as in Examples 1–3. As may have been anticipated, the time to appearance of lacunae decreases monotonically as α , hence also s_n , increases; our results quantify the exact relationship. \blacksquare

C Proof Sketch

The proof of the main theorem follows ideas laid out in [18]. While the ideas are very simple they tend to be obscured by a very considerable amount of technical detail. We hence

provide a skein of the key steps so that the simple nature of the proof may be appreciated; the complete proof is presented in Section 5. For simplicity, consider point isolation, $\ell = 0$. Then the main theorem says that, under the conditions (1), ${}^0N(t_n; r_n, c_n)$ converges in distribution to $Po(\lambda)$, the Poisson distribution with mean λ .

For the nonce suppress the subscripts n and c and write $r = r_n$, $t = t_n$, $F(t) = F_{c_n}(t_n)$, and $G(t) = G_{c_n}(t_n)$. Consider any vertex X_i . Let A denote the area of the intersection of the unit circle with the circle of radius r centred at the vertex. If X_i is in the interior of the unit circle, i.e., $|X_i| \leq 1 - r$, then A is identically πr^2 . If X_i is in the boundary of the unit circle, i.e., $1 - r < |X_i| \leq 1$, then $A < \pi r^2$. The probability that X_i lies in the interior is $\pi(1 - r)^2/\pi = (1 - r)^2 = 1 + \mathcal{O}(r)$ whence the probability that X_i lies in the boundary is $1 - (1 - r)^2 = \mathcal{O}(r)$. If r is suitably small this suggests that the contribution of the boundary may be sub-dominant and, indeed, this turns out to be the case though the details are messy and non-trivial (the conclusion is false in three or more dimensions and for r_n of order larger than that prescribed in (1)).

Accordingly, focus on contributions from the interior of the unit circle. The claimed result follows from the following observations.

1° *Vertex isolations are rare.* More precisely, condition on X_i being in the interior of the unit circle. The probability that any given vertex X_j is adjacent to X_i is then simply $\pi r^2/\pi = r^2$. As the vertices are placed independently, the probability that X_i has k vertices adjacent to it is given by the binomial $\binom{n-1}{k}(r^2)^k(1 - r^2)^{n-1-k}$ and the probability that they are all extinguished by time t is $F(t)^k$. It follows that the (conditional) probability that X_i is isolated at time t is given by

$$\sum_{k=0}^{n-1} \binom{n-1}{k} (r^2)^k (1 - r^2)^{n-1-k} F(t)^k = (r^2 F(t) + 1 - r^2)^{n-1} = (1 - r^2 G(t))^{n-1}$$

as could also have been directly deduced. Now observe that $n r^4 G(t)^2 \rightarrow 0$ for the range of $r = r_n$ and $t = t_n$ given in (1) (with ℓ_n set to 0). It follows that the right-hand side is asymptotic to $e^{-n r^2 G(t)} \sim \lambda/n$. Remove the conditioning by taking expectations and as the boundary condition is sub-dominant obtain that the probability that vertex X_i is isolated at time t in the graph $\mathcal{G}_{n,r}$ is asymptotic to λ/n .

This estimate is very useful because of the observation:

2° *Vertex isolations are asymptotically independent.* Fix k and observe that for specified vertices X_{i_1}, \dots, X_{i_k} , the probability that the circles of radius r at each of the locations X_{i_j} are mutually non-overlapping is $\geq (1 - 4r^2)(1 - 8r^2) \dots (1 - (k-1)4r^2) = 1 + \mathcal{O}(r^2)$. It is plausible now, and is indeed the case, that this is the dominant term though the details are delicate and complicated by pervasive dependencies and boundary effects; we eschew the rigorous considerations here. Conditioned on mutually non-overlapping circles at the vertices, the probability that each of X_{i_1}, \dots, X_{i_k} is isolated is then given by $(1 - k r^2 G(t))^{n-k}$ which in turn is asymptotic to λ^k/n^k for the stated conditions. Vertex isolations hence, as claimed, exhibit an asymptotic independence property.

This observation allows us to finish off the proof via the aphorism:

3° *Weakly dependent rare events have an asymptotic Poisson distribution.* Indeed, to make the observation somewhat more precise, let ${}^0L_{i_1}(t)$ denote the event that vertex X_{i_1} is isolated at time t in the graph $\mathcal{G}_{n,r}$ and, for each fixed positive integer k , let S_k denote the sum of all conjunctions of the events ${}^0L_{i_j}(t)$ taken k at a time, that is to say,

$$S_k = \sum_{1 \leq i_1 < \dots < i_k \leq n} \mathbf{P}({}^0L_{i_1}(t) \cap {}^0L_{i_2}(t) \cap \dots \cap {}^0L_{i_k}(t)).$$

Keep notation simple by writing ${}^0N(t) = {}^0N(t_n; r_n, c_n)$. The relevance of the sums S_k to our problem of determining the distribution of ${}^0N(t)$ is seen through the inclusion-exclusion formula,

$$\mathbf{P}\{{}^0N(t) = m\} = \sum_{k=0}^{n-m} (-1)^k \binom{m+k}{m} S_{m+k},$$

so that it will suffice to estimate the S_k .

The asymptotic independence property coupled with exchangeability directly implies that $S_k = \binom{n}{k} \mathbf{P}({}^0L_1(t) \cap \cdots \cap {}^0L_k(t)) \sim \frac{n^k}{k!} \cdot \frac{\lambda^k}{n^k} = \frac{\lambda^k}{k!}$. Brun's sieve (cf. Bonferroni's inequalities in Feller [6]) now shows that ${}^0N(t)$ tends in distribution to the Poisson with mean λ to finish off the proof. \blacksquare

4 Technical Results

Before proceeding to the proof of the theorem let us collect all the technical results we will need for easy reference. We begin with three easy, elementary inequalities; the proofs follow from routine Taylor arguments and are sketched only for completeness.

LEMMA 1 *Bounds for elementary functions.*

- a. *Arc sine:* $\arcsin x \geq x$ for $0 \leq x \leq 1$ and $\arcsin x \leq x + x^3 \leq 2x$ for $0 \leq x \leq 0.6083$.
- b. *Exponential:* $1 + x \leq e^x$ for all x and $e^x = 1 + x + \mathcal{O}(x^2)$ as $x \rightarrow 0$.
- c. *Logarithm:* $\log(1 - x) = -x + \mathcal{O}(x^2)$ as $x \rightarrow 0$. In particular, $(1 - x)^a = 1 - ax + \mathcal{O}(x^2)$ as $x \rightarrow 0$ for every real a .

PROOF: (a) Write $f(x) = \arcsin x$. Then $f'(x) = (1 - x^2)^{-1/2}$, $f''(x) = x(1 - x^2)^{-3/2}$, and $f'''(x) = (1 - x^2)^{-3/2} + 3x^2(1 - x^2)^{-5/2}$. As f''' is never negative it follows that f'' is monotone increasing. Taylor's theorem with remainder says that $f(x) = f(0) + f'(0)x + f''(x_0)x^2/2 = x + f''(x_0)x^2/2$ for some x_0 between 0 and x . As $f''(t) = t(1 - t^2)^{-3/2} \geq 0$ for all t in the unit interval it follows that $f(x) = \arcsin x \geq x$ establishing the claimed lower bound. On the other hand, $x_0 \leq x$ whence $f''(x_0) \leq f''(x)$. It follows that $f(x) \leq x + f''(x)x^2/2 = x + x^3/2(1 - x^2)^{3/2} \leq x + x^3$ provided $x \leq \sqrt{1 - 2^{-2/3}} = 0.6083 \dots$. And of course $x^3 \leq x$ if $0 \leq x \leq 1$ to finish off the proof.

(b) Write $g(x) = e^x$. Taylor's theorem with remainder yields $g(x) = g(0) + g'(0)x + g''(x_0)x^2/2$ for some x_0 lying between 0 and x . It follows that $e^x = 1 + x + e^{x_0}x^2/2 \geq 1 + x$ as e^t is positive for all t . The asymptotic expansion for the exponential follows quickly from the observation that if the complete Taylor series for the exponential $e^x = \sum_{k=0}^{\infty} x^k/k!$ is truncated after two terms, the error in the approximation is bounded in absolute value by

$$\sum_{k=2}^{\infty} \frac{|x|^k}{k!} \leq \frac{x^2}{2} \sum_{k=2}^{\infty} |x|^{k-2} = \frac{x^2}{2(1 - |x|)} \leq x^2$$

if $|x| \leq 1/2$.

(c) The Taylor series for the logarithm gives $\log(1 - x) = -\sum_{k=1}^{\infty} \frac{x^k}{k}$ for $|x| < 1$. Truncating the series after one term results in an approximation error bounded in absolute value by

$$\sum_{k=2}^{\infty} \frac{|x|^k}{k} \leq \frac{x^2}{2} \sum_{k=2}^{\infty} |x|^{k-2} = \frac{x^2}{2(1 - |x|)} \leq x^2$$

again if $|x| \leq 1/2$. Finally, write $(1-x)^\alpha = e^{\alpha \log(1-x)}$ and apply the asymptotic estimates for the exponential and the logarithm to complete the proof of the assertion. \blacksquare

Refinements of standard inclusion-exclusion arguments go by the collective name of Bonferroni's inequalities (cf. Feller [6]). We will use the following variant.

Suppose A_1, \dots, A_n are events in a probability space and let P_m denote the probability of the event that exactly m of the A_i occur. The inclusion-exclusion formula then gives us the explicit result

$$P_m = \sum_{k=0}^{n-m} (-1)^k \binom{m+k}{m} S_{m+k} \quad (3)$$

where S_k is the sum of all the probabilities of conjunctions of the events A_i , k at a time. It will be convenient to introduce the notation

$$f_m(K) = \sum_{k=0}^{K-1} (-1)^k \binom{m+k}{m} S_{m+k}$$

for the truncated sums of the inclusion-exclusion formula. Clearly, $f_m(n-m+1) = P_m$, but much more can be said.

LEMMA 2 *The truncated sums $f_m(K)$ form an increasingly fine series of approximations to P_m and bound P_m from below when K is even and from above when K is odd. More precisely, the approximation error $P_m - f_m(K)$ has the sign $(-1)^K$ of the first neglected term in the inclusion-exclusion formula (3) and is bounded in absolute value by that term.*

PROOF: We sketch a short proof for completeness. Consider the family of events of the form $E = B_1 \cap \dots \cap B_n$ where each B_i is either A_i or A_i^c . This family of events partitions the sample space Ω and *a fortiori* partitions each A_i and A_i^c . Each event E in this family is hence either contained in any given A_i or is disjoint from it, i.e., is contained in A_i^c . In other words, $E \cap A_i$ is either E or \emptyset . Suppose E is contained in exactly $m+L$ of the A_i where $-m \leq L = L(E) \leq n-m$. As

$$P_m - f_m(K) = \sum_{k \geq K} (-1)^k \binom{m+k}{m} S_{m+k}, \quad (4)$$

the contribution of E to the sum on the right is identically 0 if $L < K$ (as $S_{m+k} = 0$ if $k > L$). Now suppose $L \geq K$. Then the contribution of E to the sum is given by

$$\begin{aligned} \mathbf{P}(E) \sum_{k \geq K} (-1)^k \binom{m+k}{k} \binom{m+L}{m+k} &= \mathbf{P}(E) \binom{m+L}{m} \sum_{k \geq K} (-1)^k \binom{L}{k} \\ &= \mathbf{P}(E) \binom{m+L}{m} \sum_{k \geq K} (-1)^k \left[\binom{L-1}{k} + \binom{L-1}{k-1} \right], \end{aligned}$$

the last step following by an application of Pascal's triangle. The sum on the right telescopes with terms cancelling pairwise leaving only the term $(-1)^K \binom{L-1}{K-1}$. The contribution of E to the right-hand side of (4) is hence $(-1)^K \binom{m+L}{m} \binom{L-1}{K-1} \mathbf{P}(E)$ which, it may be observed, is less in absolute value than $\binom{m+L}{m} \binom{L}{K} \mathbf{P}(E)$, the absolute value of the contribution of E to the first term that has been left out of the truncated series. As each event E contributes either 0 or a term of sign $(-1)^K$ to the right-hand side of (4), it follows that $P_m - f_m(K) = (-1)^K C_K$ where C_K is a non-negative constant satisfying $C_K \leq \binom{m+K}{m} S_{m+K}$. \blacksquare

5 Proofs

The specification of the lacuna radius ℓ_n plays no essential rôle in the structure of the proof of the main theorem, though of course the particular choice affects the critical time t_n at which isolated discs $\mathbb{D}_i(\ell_n)$ first emerge in the graph \mathcal{G}_{n,r_n} . We simplify presentation accordingly by considering first the case $\ell_n = 0$. The setting is now that of isolated vertices in the graph \mathcal{G}_{n,r_n} and with $R_n = r_n$ the conditions (1) become

$$r_n = o\left(\frac{\log n}{\sqrt{n}}\right) \quad \text{and} \quad r_n^2 G_{c_n}(t_n) = \frac{1}{n} \log \frac{n}{\lambda} + o\left(\frac{1}{n}\right) \quad (1'')$$

as $n \rightarrow \infty$. Before proceeding observe that these conditions imply that $e^{-nr_n^2 G_{c_n}(t_n)} \sim \frac{\lambda}{n}$, $nr_n^3 G_{c_n}(t_n) = \mathcal{O}(r_n \log n) = o\left(\frac{\log^2 n}{\sqrt{n}}\right)$, and $nr_n^4 G_{c_n}^2(t_n) = \mathcal{O}\left(\frac{\log^2 n}{n}\right)$.

The main theorem specialised to this setting says that under the conditions (1'') the number of isolated vertices at time t_n in the graph \mathcal{G}_{n,r_n} converges in distribution to the Poisson with mean λ .

As will become apparent, the proof for the general case will carry through with little more than the systematic replacement of r_n by $R_n = \sqrt{2\ell_n r_n + r_n^2}$ in the following development.

To keep the notational mess under control we will from now on suppress subscripts when it is possible to do so without confusion; for instance, we write $r = r_n$, $t = t_n$, and $G(t) = G_{c_n}(t_n)$. We also suppress the rôles of r_n and c_n and write simply ${}^0N(t) = {}^0N(t_n; r_n, c_n)$ for the number of isolated vertices at time $t = t_n$ in the graph \mathcal{G}_{n,r_n} .

It will be useful to set up some additional notation at this stage. As before, write ${}^0L_i(t)$ for the event that vertex X_i is isolated by time $t = t_n$ in the graph \mathcal{G}_{n,r_n} and, in an extension of this notation, ${}^0L_{i_1, \dots, i_k}(t)$ for the event that vertices X_{i_1}, \dots, X_{i_k} are all isolated by time t . Write ${}^0P(t) = \mathbf{P}({}^0L_i(t))$ for the probability that vertex X_i is isolated by time t ; by symmetry, this probability does not depend upon the choice of i though there is of course an implicit dependence on n . It follows that $\mathbf{E}\{{}^0N(t)\} = n\{{}^0P(t)\}$.

Under the conditions (1'') we will show that:

- 1° *Vertex isolations are rare*, or more precisely, ${}^0P(t) \sim \frac{\lambda}{n}$.
- 2° Moreover, *vertex isolations are weakly asymptotically independent*, to wit, $\mathbf{P}({}^0L_{i_1, \dots, i_k}(t)) \sim [{}^0P(t)]^k \sim \frac{\lambda^k}{n^k}$ for every fixed positive integer k .
- 3° And finally, *aberrant vertices are trapped in a Poisson sieve*, or more formally, $\mathbf{P}\{{}^0N(t) = m\} \rightarrow e^{-\lambda} \frac{\lambda^m}{m!}$ for every nonnegative integer m .

It will be natural to separate the proof into these three main stages.

1° SINGLE VERTEX ISOLATION. We begin by considering the progress of a single vertex, say X_i , towards isolation. This is the key to the proof and the results of the analysis will be in repeated use in subsequent stages.

Recall that the points X_1, \dots, X_n are generated by independent sampling from the uniform distribution in the unit circle in the Euclidean plane. The unit circle hence comprises the *sensor field*. In the graph $\mathcal{G}_{n,r}$, vertices adjacent to X_i must lie in the region defined by the intersection of the unit circle with the circle of radius r centred at X_i . We call this the *region of visibility* of vertex X_i . By symmetry it is clear that the area $A = A(X_i)$ of the region of visibility depends only on the distance of X_i from the origin. See Figure 1.

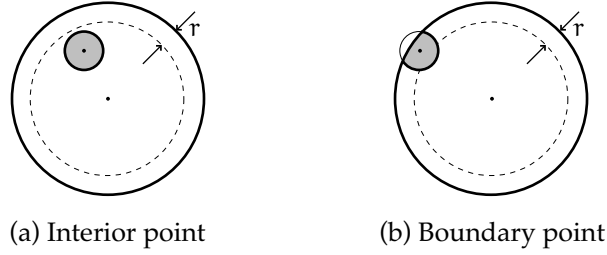


Figure 1: Two cases for the region of visibility (shown shaded). (a) X_i lies in the interior of the unit circle. (b) X_i lies in an annulus of width r at the boundary of the unit circle.

Given X_i , the conditional probability that any other vertex X_j is adjacent to X_i is given by $a(X_i) = A(X_i)/\pi$ so that the number of vertices adjacent to X_i corresponds to the number of successes in $n - 1$ tosses of a bent coin with success probability $a(X_i)$. As each vertex progresses to failure independently with common distribution function $F(t) = F_{c_n}(t)$ for the time to failure, given X_i the conditional probability that vertex X_i is isolated by time t in $\mathcal{G}_{n,r}$ satisfies

$$\begin{aligned} \mathbf{P}({}^0L_i(t) \mid X_i) &= \sum_{k=0}^{n-1} \binom{n-1}{k} a(X_i)^k (1 - a(X_i))^{n-1-k} F(t)^k \\ &= [a(X_i)F(t) + (1 - a(X_i))]^{n-1} = (1 - a(X_i)G(t))^{n-1} \end{aligned}$$

where, as before, $G(t) = 1 - F(t)$ is the right tail of the lifetime distribution. Take expectation with respect to X_i to get rid of the conditioning and obtain

$${}^0P(t) = \mathbf{E}\{\mathbf{P}({}^0L_i(t) \mid X_i)\} = \mathbf{E}\{(1 - a(X_i)G(t))^{n-1}\}. \quad (5)$$

Henceforth we will suppose that $r = r_n$, $c = c_n$, and $t = t_n$ satisfy the theorem conditions (1'').

Some preliminary spadework helps put subsequent expressions into an analytically amenable framework. Observe that $A(X_i) \leq \pi r^2$ whence $a(X_i) \leq r^2$ with equality in the interior of the unit circle. As $\log(1 - x) = -x + \mathcal{O}(x^2)$ and $e^x = 1 + \mathcal{O}(x)$ as $x \rightarrow 0$, an easy application of Lemma 1 now shows that

$$\begin{aligned} (1 - a(X_i)G(t))^{n-1} &= e^{n \log(1 - a(X_i)G(t))} (1 - a(X_i)G(t))^{-1} \\ &= e^{-na(X_i)G(t) + \mathcal{O}(nr^4 G^2(t))} [1 + \mathcal{O}(r^2 G(t))] = e^{-na(X_i)G(t)} [1 + \mathcal{O}(\frac{\log^2 n}{n})] \end{aligned}$$

where the order bound is uniform in X_i . It follows that

$${}^0P(t) = [1 + \mathcal{O}(\frac{\log^2 n}{n})] \mathbf{E}(e^{-na(X_i)G(t)}) \quad (n \rightarrow \infty) \quad (6)$$

and it suffices hence to evaluate

$$I(n) \triangleq \mathbf{E}(e^{-na(X_i)G(t)}) = \frac{1}{\pi} \int e^{-na(x_i)G(t)} dx_i \quad (6')$$

where the integral ranges over all points in the unit disc $\mathbb{D}_i(1;0) = \{x_i : |x_i| \leq 1\}$.³

³The words disc and circle are used interchangeably for our purposes.

The observation that $A(X_i)$, hence also $a(X_i)$, depends only on the distance $|X_i|$ of vertex X_i from the origin helps further simplify the expression. The distance $|X_i|$ of vertex X_i from the field centre is a random variable with distribution function $\mathbf{P}\{|X_i| \leq \rho\} = \pi\rho^2/\pi = \rho^2$ for $0 \leq \rho \leq 1$. It follows that $|X_i|$ has density 2ρ ($0 \leq \rho \leq 1$). In a slight abuse of notation, write $a(X_i) = a_{|X_i|}$ to emphasise the dependence of a on the length of X_i alone. We hence have

$$I(n) = \mathbf{E}(e^{-na_{|X_i|}G(t)}) = \int_0^1 2\rho e^{-na_\rho G(t)} d\rho.$$

It is expedient to partition the range of the integral and write $I(n) = I_{\text{interior}} + I_{\text{boundary}}$ where I_{interior} is the contribution to the integral from the interior of the unit circle $0 \leq \rho \leq 1-r$ and I_{boundary} is the contribution to the integral from the annulus $1-r < \rho \leq 1$ at the boundary. We evaluate these contributions in turn.

The interior contribution. When $0 \leq \rho \leq 1-r$, the point X_i is in the interior of the unit circle and the circle of radius r centred at X_i is contained wholly within the sensor field as illustrated in Figure 1(a). It follows that $a_\rho = \pi r^2/\pi = r^2$ whence

$$I_{\text{interior}} = \int_0^{1-r} 2\rho e^{-na_\rho G(t)} d\rho = e^{-nr^2 G(t)} (1-r)^2 = e^{-nr^2 G(t)} [1 + \mathcal{O}(\frac{\log n}{\sqrt{n}})] \sim \frac{\lambda}{n}$$

asymptotically as $n \rightarrow \infty$.

The boundary contribution. When $1-r < \rho \leq 1$, the point X_i lies in an asymptotically vanishing annulus of width r at the boundary of the unit circle. The region of visibility is now a lens as shown in the shaded region in Figure 1(b) and it is clear that a_ρ decreases monotonically from r^2 to a value close to $r^2/2$ as ρ increases from $1-r$ to 1. We cannot simply ignore losses at the boundary, tempting as it is to do so, as an isolated vertex on the boundary will result in a significant sensory lacuna in the sensor field, the size of the lacuna being at least half that of a lacuna at an isolated vertex in the interior.

The situation at the boundary is extremely delicate. On the face of it, the probability that a vertex lands in the boundary is small so that other things being equal the boundary should contribute very little to the probability of isolation. However, in the boundary annulus the area of a vertex's region of visibility is about one-half of its area in the interior, in consequence fewer vertices are adjacent to it, and hence the chances of isolation increase as isolation now requires the extinction of fewer vertices than in the interior. The contribution to the probability of isolation from the boundary is dynamically balanced between these two opposing effects, the critical factor being the rate of decrease of the radius of communication $r = r_n$ with n . As we shall see, the given rate $r_n = o(\frac{\log n}{\sqrt{n}})$ is essentially best possible for the stated results to hold.

There are two geometrically distinct regimes in the boundary depending on whether X_i and the origin lie on the same side of the chord joining the intersections of the two circles or whether X_i and the origin are separated by the chord. Two typical situations are illustrated in Figure 2 where the small circle of radius r has been grossly exaggerated in size to make the details visible. Here X_i is located at point Q.

The contribution of the boundary to the probability integral may hence be further decomposed into $I_{\text{boundary}} = I_{\text{boundary}}^{(1)} + I_{\text{boundary}}^{(2)}$ where

$$I_{\text{boundary}}^{(1)} = \int_{1-r}^{\sqrt{1-r^2}} 2\rho e^{-na_\rho G(t)} d\rho \quad \text{and} \quad I_{\text{boundary}}^{(2)} = \int_{\sqrt{1-r^2}}^1 2\rho e^{-na_\rho G(t)} d\rho$$

are the near- and far-boundary contributions, respectively. We consider these in turn.

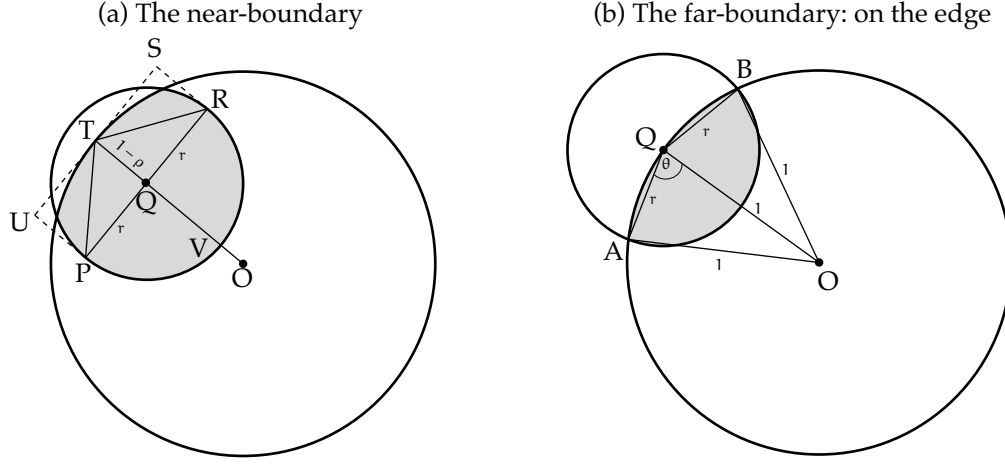


Figure 2: The boundary regime and the visibility lens (shown shaded) with X_i located at point Q. (a) The vertex is located in the near-boundary $1 - r < \rho \leq \sqrt{1 - r^2}$. (b) The vertex is located at the very edge of the far-boundary $\sqrt{1 - r^2} < \rho \leq 1$.

The near-boundary: $1 - r < \rho \leq \sqrt{1 - r^2}$. This is the critical region where the boundary effects are most pronounced. Consider the typical situation illustrated in Figure 2(a). While the calculation of lens area is now routine, if tedious, we can finesse some of these calculations by bounding the dominant contribution though some care needs to be exercised as the asymptotics are delicate.

On the one hand, the conjoined area encompassed by the semicircle PQRVP and the isosceles triangle PTR is wholly contained within the lens while, on the other, the conjoined area encompassed by the semicircle PQRVP and the rectangle PUSR contains the entire lens. It follows that the area of the lens, A_ρ , is bounded below and above, respectively, by these conjoined areas. An easy calculation now shows that

$$\frac{1}{2}\pi r^2 + r(1 - \rho) < A_\rho < \frac{1}{2}\pi r^2 + 2r(1 - \rho)$$

and, consequently, the probability $\alpha_\rho = \frac{1}{\pi}A_\rho$ that a randomly placed vertex will land in the lenticular area at the near-boundary is bounded by

$$\frac{1}{2}r^2 + \frac{1}{\pi}r(1 - \rho) < \alpha_\rho < \frac{1}{2}r^2 + \frac{2}{\pi}r(1 - \rho). \quad (7)$$

The lower bound for α_ρ may be immediately deployed in bounding the contribution of the near-boundary to the probability integral via

$$\begin{aligned} I_{\text{boundary}}^{(1)} &\stackrel{(i)}{\leq} e^{-nr^2 G(t)/2} \int_{1-r}^{\sqrt{1-r^2}} 2\rho e^{-nrG(t)(1-\rho)/\pi} d\rho \\ &\stackrel{(ii)}{\leq} 2e^{-nr^2 G(t)/2} \int_{1-r}^{\sqrt{1-r^2}} e^{-nrG(t)(1-\rho)/\pi} d\rho \\ &\stackrel{(iii)}{=} 2e^{-nr^2 G(t)/2} \int_{1-\sqrt{1-r^2}}^r e^{-nrG(t)u/\pi} du \\ &\leq 2e^{-nr^2 G(t)/2} \int_0^\infty e^{-nrG(t)u/\pi} du \end{aligned}$$

$$= \frac{2\pi e^{-nr^2 G(t)/2}}{nrG(t)} \sim \frac{2\pi r\sqrt{\lambda}}{\sqrt{n} \log n} \quad (n \rightarrow \infty)$$

where (i) follows from the lower bound (7) for a_ρ , (ii) holds because ρ is trivially bounded above by $\sqrt{1-r^2} \leq 1$ inside the integral, and (iii) follows from a change of variable of integration from ρ to $u = 1 - \rho$. We hence obtain the asymptotic estimate

$$I_{\text{boundary}}^{(1)} = \mathcal{O}\left(\frac{r}{\sqrt{n} \log n}\right) = o\left(\frac{1}{n}\right) \quad (n \rightarrow \infty)$$

by virtue of the growth condition $r = r_n = o\left(\frac{\log n}{\sqrt{n}}\right)$. It follows that the contribution from the near-boundary to the isolation probability is dominated asymptotically by the interior contribution $I_{\text{interior}} \sim \frac{\lambda}{n}$.

That the rate for r cannot be further increased may be seen from the upper bound for a_ρ in (7). An entirely similar calculation to that above shows that

$$\begin{aligned} I_{\text{boundary}}^{(1)} &\geq e^{-nr^2 G(t)/2} \int_{1-r}^{\sqrt{1-r^2}} 2\rho e^{-2nrG(t)(1-\rho)/\pi} d\rho \\ &\geq 2(1-r)e^{-nr^2 G(t)/2} \int_{1-r}^{\sqrt{1-r^2}} e^{-2nrG(t)(1-\rho)/\pi} d\rho \\ &= \frac{\pi(1-r)e^{-nr^2 G(t)/2}}{nrG(t)} [e^{-2nrG(t)(1-\sqrt{1-r^2})/\pi} - e^{-2nr^2 G(t)/\pi}] \\ &\stackrel{\text{(iv)}}{=} \frac{\pi e^{-nr^2 G(t)/2}}{nrG(t)} (1-r) [1 + \mathcal{O}(r \log n) + \mathcal{O}(n^{-2/\pi})] \\ &= \frac{\pi e^{-nr^2 G(t)/2}}{nrG(t)} [1 + o\left(\frac{\log^2 n}{\sqrt{n}}\right)] \sim \frac{\pi r\sqrt{\lambda}}{\sqrt{n} \log n} \quad (n \rightarrow \infty) \end{aligned}$$

where (iv) follows as a consequence of the asymptotic estimate $1 - \sqrt{1-r^2} = r^2/2 + \mathcal{O}(r^4)$. It follows that $I_{\text{boundary}}^{(1)}$ is *exactly* of the asymptotic order of $r/\sqrt{n} \log n$. If $r = r_n$ were to have an asymptotic rate of the order of or higher than $\log n/\sqrt{n}$ then the contribution from the boundary is at least comparable to the interior contribution $I_{\text{interior}} \sim \frac{\lambda}{n}$ and the boundary comes into play.

The far-boundary: $\sqrt{1-r^2} < \rho \leq 1$. Recall that a_ρ decreases monotonically as ρ increases so that $a_\rho \geq a_1 = \frac{1}{\pi} A_1$ where A_1 is the area of the visibility lens when X_i is situated on the circumference of the unit circle. The situation is illustrated in Figure 2(b) where the small circle of radius r has again been grossly exaggerated to make visible the geometric detail.

With notation as in Figure 2(b), $\theta = \angle A Q O$ is the half-angle of the sector enclosed by the chords AQ and BQ and the interior rim of the circle of radius r centred at Q on the circumference of the unit circle. Write A_{sector} for the area of this sector. It follows that $A_{\text{sector}} = \frac{1}{2}(2\theta)r^2 = \theta r^2$. As $A O Q$ is an isosceles triangle with side 1 and base r , we have $\theta = \arccos\left(\frac{r}{2}\right) = \frac{\pi}{2} - \arcsin\left(\frac{r}{2}\right)$. In consequence of the bound $\arcsin x \leq 2x$ for sufficiently small x (Lemma 1(a)) we then obtain

$$a_1 = \frac{1}{\pi} A_1 \geq \frac{1}{\pi} A_{\text{sector}} = \frac{1}{2} r^2 - \frac{1}{\pi} r^2 \arcsin\left(\frac{r}{2}\right) \geq \frac{1}{2} r^2 - \frac{1}{\pi} r^3 \quad (8)$$

for all sufficiently large n (recall $r = r_n \rightarrow 0$). The far-boundary contribution to the proba-

bility integral may hence be bounded by

$$\begin{aligned} I_{\text{boundary}}^{(2)} &= \int_{\sqrt{1-r^2}}^1 2\rho e^{-n a_\rho G(t)} d\rho \leq \int_{\sqrt{1-r^2}}^1 2\rho e^{-n a_1 G(t)} d\rho = r^2 e^{-n a_1 G(t)} \\ &\leq r^2 e^{-\frac{1}{2} n r^2 G(t) + \frac{1}{\pi} n r^3 G(t)} = r^2 e^{-n r^2 G(t)/2} [1 + o(\frac{\log^2 n}{n})] \sim r^2 \sqrt{\frac{\lambda}{n}} \quad (n \rightarrow \infty) \end{aligned}$$

leading to the asymptotic estimate

$$I_{\text{boundary}}^{(2)} = o\left(\frac{r^2}{\sqrt{n}}\right) = o\left(\frac{\log^2 n}{n^{3/2}}\right) = o\left(\frac{1}{n}\right).$$

From the near- and far-boundary estimates we obtain the entire boundary contribution to the probability integral as⁴

$$I_{\text{boundary}} = I_{\text{boundary}}^{(1)} + I_{\text{boundary}}^{(2)} = o(n^{-1}).$$

Isolation probability. In accordance with naive expectation, the boundary contributes an asymptotically negligible amount to the isolation probability for the given maximal rate of variation of r (though the conclusion is false for rates of variation larger than prescribed). Combining the interior and boundary estimates for the integral we obtain $I(n) = I_{\text{interior}} + I_{\text{boundary}} = \frac{\lambda}{n}(1 + o(1)) + o(\frac{1}{n})$. From (6, 6') it follows that, as advertised, *the probability that any given vertex is isolated by time t in $\mathcal{G}_{n,r}$ satisfies ${}^0P(t) \sim I(n) \sim \frac{\lambda}{n}$ as $n \rightarrow \infty$* . In particular, the expected number of isolated vertices at time $t = t_n$ in $\mathcal{G}_{n,r}$ satisfies $E({}^0N(t)) \rightarrow \lambda$ as $n \rightarrow \infty$. We now proceed to refine this crude estimate.

2° CONJUNCTIONS OF VERTEX ISOLATIONS. The new features that are encountered in moving from one vertex to several vertices are statistical dependencies that arise due to overlaps of visibility regions as well as slightly more complicated boundary interactions. We will keep the burgeoning complexity under bounds by reducing considerations of dependencies that accrue for groups of vertices to repeated considerations of vertex pairs.

Let us pause here to introduce some new notation. As before, write $\mathbb{D}(z; x)$ for the closed disc of radius z centred at the point x in the plane. Let $\mathbb{S} = \mathbb{D}(1; 0)$ be the unit disc centred at the origin. This is, of course, the sensor field. We also write $\mathbb{V}(x) = \mathbb{D}(r; x) \cap \mathbb{S}$ for the region of visibility of a sensor located at point x . For brevity we say simply that $\mathbb{V}(x)$ is the region of visibility of the point x . We also define the *overlap region* of a sensor located at point x by $\mathbb{O}(x) = \mathbb{D}(2r; x) \cap \mathbb{S}$. The motivation arises from the observation that if $x_2 \in \mathbb{O}(x_1)$ then $\mathbb{V}(x_1) \cap \mathbb{V}(x_2) \neq \emptyset$ and the regions of visibility of the two points overlap. Overlap regions will be important in the characterisation of dependencies. Finally, in a slight but hopefully natural modification of an earlier notation, write $A_k(x_1, \dots, x_k) = \int_{\mathbb{V}(x_1) \cup \dots \cup \mathbb{V}(x_k)} dx$ for the area of the conjoined visibility region $\mathbb{V}(x_1) \cup \dots \cup \mathbb{V}(x_k)$ of the points x_1, \dots, x_k . Specialising to $k = 1$ and 2 , $A_1(x)$ is the area of the visibility region of point x (replacing the earlier notations $A(x)$ and $A_{|x|}$) and $A_2(x_1, x_2)$ is the area of $\mathbb{V}(x_1) \cup$

⁴It may be remarked that the analysis for the far-boundary can be applied, essentially without change, to the entire boundary contribution. While the analytical simplification is considerable it is at the cost of the much cruder estimate r/\sqrt{n} for the boundary contribution which will now be small compared to the interior contribution of order $1/n$ only if $r = r_n = o(\frac{1}{\sqrt{n}})$. This, alas!, is too small a radius of communication to guarantee connectivity and the detailed analysis of the boundary effects appears inescapable.

$\mathbb{V}(x_2)$. Finally write $a_k(x_1, \dots, x_k) = \frac{1}{\pi} A_k(x_1, \dots, x_k)$ for the probability that a randomly selected point in the unit disc \mathbb{S} falls in the region of visibility of at least one of the k points x_1, \dots, x_k . In particular, $a_1(x)$ is the probability that a randomly selected point falls in $\mathbb{V}(x)$ (replacing the earlier notations $a(x)$ and $a_{|x|}$) and $a_2(x_1, x_2)$ is the probability that a randomly selected point falls in $\mathbb{V}(x_1) \cup \mathbb{V}(x_2)$.

Fix any positive integer $k \geq 2$ and let X_{i_1}, \dots, X_{i_k} be any collection of k distinct vertices. We now proceed to estimate the probability of the event ${}^0L_{i_1, \dots, i_k}(t) = {}^0L_{i_1}(t) \cap \dots \cap {}^0L_{i_k}(t)$ that each of the k vertices X_{i_1}, \dots, X_{i_k} is isolated by time t . By symmetry, $\mathbf{P}({}^0L_{i_1, \dots, i_k}(t)) = \mathbf{P}({}^0L_{1, \dots, k}(t))$ and we may without loss of generality focus on vertices X_1 through X_k .

Given the random k -tuple of points (X_1, \dots, X_k) , the conditional probability that vertices X_1 through X_k are isolated is a random variable $\mathbf{P}({}^0L_{1, \dots, k}(t) \mid X_1, \dots, X_k)$ that takes the value $\mathbf{P}({}^0L_{1, \dots, k}(t) \mid X_1 = x_1, \dots, X_k = x_k)$ at sample points in the space characterised by the joint occurrence of the events $\{X_1 = x_1\}, \dots, \{X_k = x_k\}$. As X_1, \dots, X_n are drawn by independent sampling from the uniform distribution on the unit disc we have

$$\begin{aligned} \mathbf{P}({}^0L_{1, \dots, k}(t)) &= \mathbf{E}[\mathbf{P}({}^0L_{1, \dots, k}(t) \mid X_1, \dots, X_k)] \\ &= \frac{1}{\pi^k} \int \dots \int_{\mathbb{S}^k} \mathbf{P}({}^0L_{1, \dots, k}(t) \mid X_1 = x_1, \dots, X_k = x_k) dx_k \dots dx_1. \end{aligned} \quad (9)$$

It will again be expedient to partition the range of the integral. But first, one more definition.

The overlap graph. Every choice of points x_1, \dots, x_k in \mathbb{S} induces an *overlap graph* $\mathcal{H}_k(x_1, \dots, x_k)$ on the set of vertices $\{1, \dots, k\}$ and whose edges are all vertex pairs (i, j) for which $|x_i - x_j| \leq 2r$, that is to say, $\mathbb{V}(x_i) \cap \mathbb{V}(x_j) \neq \emptyset$. Each overlap graph $\mathcal{H}_k(x_1, \dots, x_k)$ may be partitioned into $\gamma = \gamma(x_1, \dots, x_k)$ *components* $\{\mathcal{H}_k^{(1)}, \dots, \mathcal{H}_k^{(\gamma)}\}$ where $1 \leq \gamma \leq k$ and each component $\mathcal{H}_k^{(l)}$ is a connected sub-graph with no out-going edges. (More formally, if $\mathcal{H}_k^{(l)}$ and $\mathcal{H}_k^{(m)}$ are two distinct components then \mathcal{H}_k exhibits no edges (i, j) where i is a vertex of $\mathcal{H}_k^{(l)}$ and j is a vertex of $\mathcal{H}_k^{(m)}$.)

Now any graph \mathcal{F} on the vertices $\{1, \dots, k\}$ induces an equivalence class $\mathbb{C}(\mathcal{F})$ of k -tuples of points (x_1, \dots, x_k) in \mathbb{S}^k whose overlap graph $\mathcal{H}_k(x_1, \dots, x_k)$ coincides with \mathcal{F} . As each k -tuple of points (x_1, \dots, x_k) in \mathbb{S}^k belongs to one and only one equivalence class $\mathbb{C}(\mathcal{F})$, as \mathcal{F} varies over all graphs on k vertices the sets $\mathbb{C}(\mathcal{F})$ partition \mathbb{S}^k into $2^{\binom{k}{2}}$ non-overlapping regions. We may hence partition the integral on the right-hand side of (9) and write

$$\mathbf{P}({}^0L_{1, \dots, k}(t)) = \sum_{\mathcal{F}} \mathbf{E}[1_{\mathbb{C}(\mathcal{F})}(X_1, \dots, X_k) \mathbf{P}({}^0L_{1, \dots, k}(t) \mid X_1, \dots, X_k)] \quad (10)$$

where the sum ranges over all $2^{\binom{k}{2}}$ graphs \mathcal{F} on k vertices and we use the generic indicator function notation

$$1_{\mathcal{A}}(\zeta) = \begin{cases} 1 & \text{if } \zeta \in \mathcal{A}, \\ 0 & \text{if } \zeta \notin \mathcal{A}. \end{cases}$$

Of particular interest is the graph \mathcal{F}_* obtained when the vertices $\{1, \dots, k\}$ form an independent set, that is to say, the graph has no edges. Clearly \mathcal{F}_* is the unique graph with $\gamma = k$ components, each component consisting of course of a singleton vertex. The corresponding equivalence class $\mathbb{C}(\mathcal{F}_*)$ consists of k -tuples of points (x_1, \dots, x_k) where the x_i have mutually non-overlapping regions of visibility, that is to say, $\mathbb{V}(x_i) \cap \mathbb{V}(x_j) = \emptyset$ if

$i \neq j$. The remaining graphs $\mathcal{F} \neq \mathcal{F}_*$ contain $1 \leq \gamma \leq k-1$ components and correspond to overlap graphs induced by points x_1, \dots, x_k for which at least two regions of visibility overlap. We separate these cases for consideration and write

$$\begin{aligned} J_{\text{non-overlap}} &= \mathbf{E}[1_{\mathbb{C}(\mathcal{F}_*)}(X_1, \dots, X_k) \mathbf{P}({}^0L_{1, \dots, k}(t) \mid X_1, \dots, X_k)], \\ J_{\text{overlap}} &= \sum_{\mathcal{F} \neq \mathcal{F}_*} \mathbf{E}[1_{\mathbb{C}(\mathcal{F})}(X_1, \dots, X_k) \mathbf{P}({}^0L_{1, \dots, k}(t) \mid X_1, \dots, X_k)]. \end{aligned} \quad (11)$$

Then $\mathbf{P}({}^0L_{1, \dots, k}(t)) = J_{\text{non-overlap}} + J_{\text{overlap}}$ and we proceed to evaluate these contributions in turn.

Non-overlapping regions of visibility; independent sets and the overlap graph \mathcal{F}_ .* The set of points (x_1, \dots, x_k) forming the equivalence class $\mathbb{C}(\mathcal{F}_*)$ may be systematically specified by the following recursive procedure.

BASE: The point x_1 is allowed to range over all points in the unit disc \mathbb{S} .

RECURRENCE: As j ranges from 2 to k , for every selection of x_1, \dots, x_{j-1} , the point x_j is allowed to range over the set of points $\mathbb{S} \setminus \bigcup_{i=1}^{j-1} \mathbb{O}(x_i)$ consisting of the unit disc with the overlap regions of the points x_1, \dots, x_{j-1} excised.

It is clear from the recursive construction that the points x_1, \dots, x_k specified thus have non-overlapping regions of visibility and, furthermore, a little thought shows that indeed this process covers all the points in $\mathbb{C}(\mathcal{F}_*)$. Now suppose $(x_1, \dots, x_k) \in \mathbb{C}(\mathcal{F}_*)$ so that the x_i have mutually non-overlapping regions of visibility. Then $a_k(x_1, \dots, x_k) = a_1(x_1) + \dots + a_1(x_k)$ where each $a_1(x_i) \leq r^2$ (with equality if, and only if, x_i is an interior point). Following the line of argument leading up to (5, 6) we then obtain

$$\begin{aligned} \mathbf{P}({}^0L_{1, \dots, k}(t) \mid X_1 = x_1, \dots, X_k = x_k) &= (1 - a_k(x_1, \dots, x_k)G(t))^{n-k} \\ &= [1 + \mathcal{O}(\frac{\log^2 n}{n})] e^{-n a_k(x_1, \dots, x_k)G(t)} = [1 + \mathcal{O}(\frac{\log^2 n}{n})] \prod_{j=1}^k e^{-n a_1(x_j)G(t)} \end{aligned}$$

where the order term is uniform over all choices of x_1, \dots, x_k . By systematically conditioning on X_1 first, then X_2 , and so on, and finally conditioning on X_k , we obtain

$$\begin{aligned} J_{\text{non-overlap}} &= [1 + \mathcal{O}(\frac{\log^2 n}{n})] \mathbf{E} \left(1_{\mathbb{C}(\mathcal{F}_*)}(X_1, \dots, X_k) \prod_{j=1}^k e^{-n a_1(X_j)G(t)} \right) \\ &= [1 + \mathcal{O}(\frac{\log^2 n}{n})] \frac{1}{\pi} \int_{\mathbb{S}} dx_1 e^{-n a_1(x_1)G(t)} \frac{1}{\pi} \int_{\mathbb{S} \setminus \mathbb{O}(x_1)} dx_2 e^{-n a_1(x_2)G(t)} \\ &\quad \dots \frac{1}{\pi} \int_{\mathbb{S} \setminus \bigcup_{i=1}^{k-1} \mathbb{O}(x_i)} dx_k e^{-n a_1(x_k)G(t)}. \end{aligned}$$

A typical nested integral on the right-hand side is of the form

$$\frac{1}{\pi} \int_{\mathbb{S} \setminus \bigcup_{i=1}^{j-1} \mathbb{O}(x_i)} dx_j e^{-n a_1(x_j)G(t)} = \frac{1}{\pi} \int_{\mathbb{S}} dx_j e^{-n a_1(x_j)G(t)} - \frac{1}{\pi} \int_{\bigcup_{i=1}^{j-1} \mathbb{O}(x_i)} dx_j e^{-n a_1(x_j)G(t)}.$$

The first integral on the right is, up to a multiplicative factor of $1 + o(1)$, just the probability that vertex X_j is isolated by time t in $\mathcal{G}_{n,r}$ (see (6, 6')) whence

$$\frac{1}{\pi} \int_{\mathbb{S}} dx_j e^{-n a_1(x_j)G(t)} \sim {}^0P(t) \sim \frac{\lambda}{n} \quad (n \rightarrow \infty)$$

from our considerations for a single vertex. As $a_1(x_j) \geq \frac{1}{2}r^2 - \frac{1}{\pi}r^3$ for large enough n (see (8)), the second of the two integrals on the right is bounded by

$$\begin{aligned} & \frac{1}{\pi} \int_{\bigcup_{i=1}^{j-1} \mathbb{O}(x_i)} dx_j e^{-na_1(x_j)G(t)} \\ & \leq e^{-\frac{1}{2}nr^2G(t) + \frac{1}{\pi}nr^3G(t)} \left(\frac{1}{\pi} \int_{\bigcup_{i=1}^{j-1} \mathbb{O}(x_i)} dx_j \right) \leq (j-1)4r^2 e^{-\frac{1}{2}nr^2G(t) + \frac{1}{\pi}nr^3G(t)} \\ & = (j-1)4r^2 \sqrt{\frac{\lambda}{n}} (1 + o(1)) (1 + \mathcal{O}(r \log n)) = \mathcal{O}\left(\frac{r^2}{\sqrt{n}}\right) = o\left(\frac{\log^2 n}{n^{3/2}}\right) \end{aligned}$$

where the order term is uniform with respect to the x_i . Consequently,

$$\frac{1}{\pi} \int_{\mathbb{S} \setminus \bigcup_{i=1}^{j-1} \mathbb{O}(x_i)} dx_j e^{-na_1(x_j)G(t)} = \frac{\lambda}{n} \left[1 + o(1) + o\left(\frac{\log^2 n}{\sqrt{n}}\right) \right] \quad (12)$$

for each j and we obtain the estimate

$$J_{\text{non-overlap}} = \frac{\lambda^k}{k!} \left[1 + o(1) + o\left(\frac{\log^2 n}{\sqrt{n}}\right) + \mathcal{O}\left(\frac{\log^2 n}{n}\right) \right] \sim \frac{\lambda^k}{n^k} \quad (13)$$

asymptotically as $n \rightarrow \infty$.

Overlapping regions of visibility preliminaries; connected overlap graphs. We may systematically group graphs \mathcal{F} on k vertices according to (i) the number of components $\gamma = \gamma(\mathcal{F})$ of the graph and (ii) the sizes of the components k_1, \dots, k_γ . Define

$$J_{k_1, \dots, k_\gamma} \triangleq \sum_{\mathcal{F}_{k_1, \dots, k_\gamma}} \mathbb{E} \left[\mathbb{1}_{\mathbb{C}(\mathcal{F}_{k_1, \dots, k_\gamma})}(X_1, \dots, X_k) \mathbf{P}({}^0L_{1, \dots, k}(t) \mid X_1, \dots, X_k) \right] \quad (14)$$

where, in an obvious notation, the sum on the right ranges over all graphs $\mathcal{F}_{k_1, \dots, k_\gamma}$ with γ components of sizes k_1, \dots, k_γ .⁵ As graphs in the family $\{\mathcal{F} : \mathcal{F} \neq \mathcal{F}_*\}$ have a number of components varying between $1 \leq \gamma \leq k-1$ we accordingly obtain

$$J_{\text{overlap}} = \sum_{\gamma=1}^{k-1} \sum_{\substack{k_1 \geq \dots \geq k_\gamma \geq 1 \\ k_1 + \dots + k_\gamma = k}} J_{k_1, \dots, k_\gamma}. \quad (14')$$

Begin by considering the cases when the overlap graphs consist of a single component, $\gamma = 1$. Of course, in these cases, the graphs themselves are connected and the single component has size k . As we shall see, this case informs all the others.

Specialising to the case $\gamma = 1$, (14) becomes

$$J_k = \sum_{\mathcal{F}_k} \mathbb{E} \left[\mathbb{1}_{\mathbb{C}(\mathcal{F}_k)}(X_1, \dots, X_k) \mathbf{P}({}^0L_{1, \dots, k}(t) \mid X_1, \dots, X_k) \right] \quad (15)$$

where \mathcal{F}_k now ranges over all *connected graphs* on k vertices. Consider any connected overlap graph \mathcal{F}_k and the associated equivalence class of k -tuples $\mathbb{C}(\mathcal{F}_k)$. As to any vertex i there is at least one vertex j such that (i, j) is an edge of \mathcal{F}_k , it follows that for any k -tuple

⁵In this new notation the graph \mathcal{F}_* may be identified with the unique graph $\mathcal{F}_{1, \dots, 1}$ but we will not be pedagogically fussy here.

$(x_1, \dots, x_k) \in \mathbb{C}(\mathcal{F}_k)$, to every point x_i there is at least one other point x_j such that the regions of visibility of x_i and x_j overlap, that is, $|x_i - x_j| \leq 2r$. If the proximity of x_i and x_j is such that indeed $|x_i - x_j| \leq r$ then vertices X_i and X_j will be adjacent to each other in the original graph $\mathcal{G}_{n,r}$. It follows that conditioned on $\{X_1 = x_1, \dots, X_k = x_k\}$, the occurrence of the event ${}^0L_{1,\dots,k}(t)$ will require not only that any of the vertices X_{k+1}, \dots, X_n that fall in the conjoined visibility region $\mathbb{V}(x_1) \cup \dots \cup \mathbb{V}(x_k)$ be extinguished but may also enjoy the extinction of two or more of the vertices X_1 through X_k themselves. But in all cases we may bound

$$\begin{aligned} \mathbf{P}({}^0L_{1,\dots,k}(t) \mid X_1 = x_1, \dots, X_k = x_k) &\stackrel{(v)}{\leq} (1 - a_k(x_1, \dots, x_k)G(t))^{n-k} \\ &\stackrel{(vi)}{=} [1 + \mathcal{O}(\frac{\log^2 n}{n})] e^{-na_k(x_1, \dots, x_k)G(t)} \end{aligned} \quad (16)$$

where in (v) the inequality takes cognizance of the fact that some of the vertices from X_1 through X_k may be mutually adjacent and (vi) follows from the by-now standard process (5, 6). It follows that

$$\begin{aligned} J_k &\leq [1 + \mathcal{O}(\frac{\log^2 n}{n})] \sum_{\mathcal{F}_k} \mathbf{E}[1_{\mathbb{C}(\mathcal{F}_k)}(X_1, \dots, X_k) e^{-na_k(X_1, \dots, X_k)G(t)}] \\ &= [1 + \mathcal{O}(\frac{\log^2 n}{n})] \mathbf{E}\left[\sum_{\mathcal{F}_k} 1_{\mathbb{C}(\mathcal{F}_k)}(X_1, \dots, X_k) e^{-na_k(X_1, \dots, X_k)G(t)}\right]. \end{aligned}$$

We now begin the process of consolidating all connected overlap graphs under one rubric. Observe that $\sum_{\mathcal{F}_k} 1_{\mathbb{C}(\mathcal{F}_k)}(X_1, \dots, X_k)$ is itself the indicator for all k -tuples (X_1, \dots, X_k) for which the corresponding overlap graph is connected. Accordingly, write \mathbb{C}_k for the subset of k -tuples (x_1, \dots, x_k) in \mathbb{S}^k for which $\mathcal{H}_k(x_1, \dots, x_k)$ is connected. It then follows that $\sum_{\mathcal{F}_k} 1_{\mathbb{C}(\mathcal{F}_k)}(X_1, \dots, X_k) = 1_{\mathbb{C}_k}(X_1, \dots, X_k)$ whence

$$J_k \leq [1 + \mathcal{O}(\frac{\log^2 n}{n})] \mathbf{E}[1_{\mathbb{C}_k}(X_1, \dots, X_k) e^{-na_k(X_1, \dots, X_k)G(t)}]. \quad (17)$$

We may range over the k -tuples (x_1, \dots, x_k) in \mathbb{C}_k by allowing x_1 to range over the unit disc \mathbb{S} and, for each x_1 , allowing the $(k-1)$ -tuple (x_2, \dots, x_k) to range over the subset $\mathbb{C}_{k-1}(x_1)$ of \mathbb{S}^{k-1} for which the overlap graph $\mathcal{H}_k(x_1, \dots, x_k)$ remains connected. Now connectivity enjoins that the maximum distance from x_1 to any of the remaining points x_2, \dots, x_k can be no larger than $2(k-1)r$. It follows that the $\mathbb{C}_{k-1}(x_1)$ is contained in the set of $(k-1)$ -tuples (x_2, \dots, x_k) for which $\max_{2 \leq i \leq k} |x_i - x_1| \leq (2k-2)r$.

These considerations suggest that we introduce a new random variable Z defined by $Z = \max_{2 \leq i \leq k} |X_i - X_1|$ and representing the *diameter* of the overlap graph as viewed from X_1 . The game plan is to exploit the fact that large diameter connected graphs have relatively large footprints while small diameter connected graphs are relatively unlikely to occur while retaining bounded footprints. The latter effect is similar in flavour to the balancing act we encountered at the boundary in the analysis for a single vertex. To proceed, we now have

$$1_{\mathbb{C}_k}(X_1, \dots, X_k) = 1_{\mathbb{S}}(X_1) 1_{\mathbb{C}_{k-1}(X_1)}(X_2, \dots, X_k) \leq 1_{\mathbb{S}}(X_1) 1_{[0, (2k-2)r]}(Z)$$

so that the expectation on the right-hand side of (17) may be bounded by

$$\begin{aligned} &\mathbf{E}[1_{\mathbb{C}_k}(X_1, \dots, X_k) e^{-na_k(X_1, \dots, X_k)G(t)}] \\ &= \mathbf{E}[1_{\mathbb{S}}(X_1) \mathbf{E}(1_{\mathbb{C}_{k-1}(X_1)}(X_2, \dots, X_k) e^{-na_k(X_1, \dots, X_k)G(t)} \mid X_1)] \\ &\leq \mathbf{E}[1_{\mathbb{S}}(X_1) \mathbf{E}(1_{[0, (2k-2)r]}(Z) e^{-na_k(X_1, \dots, X_k)G(t)} \mid X_1)]. \end{aligned}$$

Now set $j^* = \arg \max_{2 \leq i \leq k} |X_i - X_1|$ and let X_{j^*} be any point at maximal distance Z from X_1 . It is clear that the conjoined area of visibility of the points X_1, \dots, X_k certainly includes the conjoined areas of visibility of the points X_1 and X_{j^*} alone so that $a_k(X_1, \dots, X_n) \geq a_2(X_1, X_{j^*})$. Substituting on the right-hand side above we may continue to bound the expectation to obtain

$$\begin{aligned} \mathbf{E}[1_{C_k}(X_1, \dots, X_k) e^{-n a_k(X_1, \dots, X_k) G(t)}] \\ \leq \mathbf{E}[1_{\mathbb{S}}(X_1) \mathbf{E}(1_{[0, (2k-2)r]}(Z) e^{-n a_2(X_1, X_{j^*}) G(t)} \mid X_1)] \triangleq K(n). \end{aligned} \quad (18)$$

The messy problem of estimating $a_k(X_1, \dots, X_k)$ for a random k -tuple is now reduced to that of estimating $a_2(X_1, X_{j^*})$ for a pair of vertices, albeit with a special statistical structure.

Following the mode of analysis for a single vertex we now partition \mathbb{S} into an interior region $\mathbb{I} = \{x : |x| \leq 1 - (2k-1)r\}$ and an (expanded) boundary annulus $\mathbb{S} \setminus \mathbb{I} = \{x : 1 - (2k-1)r < |x| \leq 1\}$. Then $1_{\mathbb{S}}(X_1) = 1_{\mathbb{I}}(X_1) + 1_{\mathbb{S} \setminus \mathbb{I}}(X_1)$ and we may partition the bound $K(n)$ on the right-hand side of (18) further into the sum of the two contributions, $K(n) = K_{\text{interior}} + K_{\text{boundary}}$, where

$$\begin{aligned} K_{\text{interior}} &= \mathbf{E}[1_{\mathbb{I}}(X_1) \mathbf{E}(1_{[0, (2k-2)r]}(Z) e^{-n a_2(X_1, X_{j^*}) G(t)} \mid X_1)] \\ K_{\text{boundary}} &= \mathbf{E}[1_{\mathbb{S} \setminus \mathbb{I}}(X_1) \mathbf{E}(1_{[0, (2k-2)r]}(Z) e^{-n a_2(X_1, X_{j^*}) G(t)} \mid X_1)]. \end{aligned} \quad (19)$$

We consider these in turn.

The interior overlap contribution: If $X_1 \in \mathbb{I}$ then the discs of radius r centred at X_1 and X_{j^*} are both wholly contained within the unit disc. As illustrated in Figure 3 there are now two possible cases depending on whether the regions of visibility of X_1 and X_{j^*} intersect.

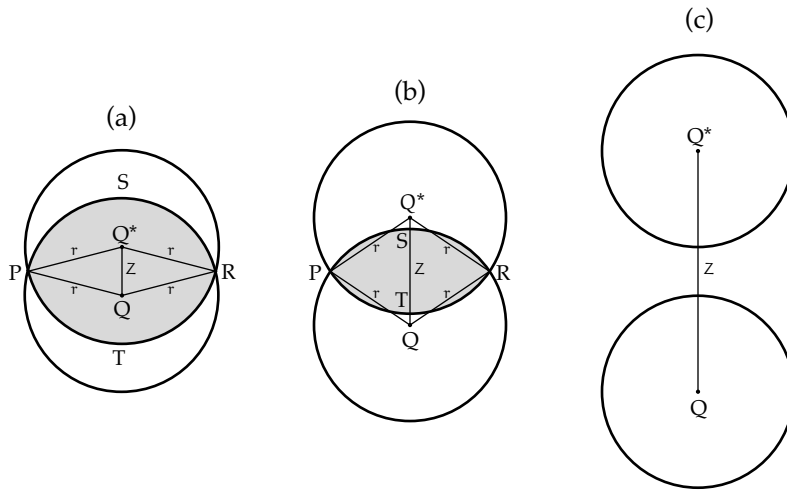


Figure 3: Point X_1 in the interior \mathbb{I} of the unit circle is located at point Q while point X_{j^*} is located at point Q^* . (a, b) Two cases where the regions of visibility of X_1 and X_{j^*} overlap. The overlap lens is shown shaded. (c) The regions of visibility of X_1 and X_{j^*} are disjoint.

CASE 1: When $0 \leq Z \leq 2r$ the regions of visibility of X_1 and X_{j^*} intersect as shown in Figures 3(a) and (b). Let A_{lens} be the area of the shaded lenticular overlap region shown in the figures. Then $A_2(X_1, X_{j^*}) = A_1(X_1) + A_2(X_2) - A_{\text{lens}} = 2\pi r^2 - A_{\text{lens}}$. Now consider the sector enclosed by the radial lines QP and QR on the one hand and the arc PSR on the

other. This sector has half-angle given by $\angle PQQ^* = \arccos\left(\frac{Z}{2r}\right) = \frac{\pi}{2} - \arcsin\left(\frac{Z}{2r}\right)$. It follows that the sector has area $A_{\text{sector}} = r^2 \angle PQQ^* = \frac{\pi}{2}r^2 - r^2 \arcsin\left(\frac{Z}{2r}\right)$. By symmetry, the sector enclosed by the radial lines Q^*P and Q^*R and the arc PTR also has area A_{sector} . The sum of the areas of these two sectors exceeds the area of the overlap lens exactly by the area of the rhombus $PQRQ^*$. While an exact calculation is not difficult we can afford to be a little cavalier here with the bound $A_{\text{lens}} \leq 2A_{\text{sector}} = \pi r^2 - 2r^2 \arcsin\left(\frac{Z}{2r}\right)$. We hence obtain

$$A_2(X_1, X_{j^*}) \geq \pi r^2 + 2r^2 \arcsin\left(\frac{Z}{2r}\right) \geq \pi r^2 + rZ$$

by virtue of the bound $\arcsin x \geq x$ (Lemma 1). In consequence,

$$\alpha_2(X_1, X_{j^*}) = \frac{1}{\pi} A_2(X_1, X_{j^*}) \geq r^2 + \frac{1}{\pi} rZ.$$

CASE 2: When $2r < Z \leq (2k-2)r$ the regions of visibility of X_1 and X_{j^*} are disjoint (Figure 3(c)) and $A_2(X_1, X_{j^*}) = A_1(X_1) + A_1(X_{j^*}) = 2\pi r^2$ whence $\alpha_2(X_1, X_{j^*}) = 2r^2$.

Write $F(z | X_1)$ and $f(z | X_1)$ for the conditional distribution function and density, respectively, of Z given X_1 . Then for all $0 \leq z \leq 1 - |X_1|$, the circle of radius z centred at X_1 is wholly contained within the unit circle so that the conditional distribution satisfies $F(z | X_1) = \mathbf{P}\{Z \leq z | X_1\} = \mathbf{P}\{|X_2 - X_1| \leq z, \dots, |X_k - X_1| \leq z | X_1\} = (z^2)^{k-1}$ as the distances $|X_i - X_1|$ ($2 \leq i \leq k$) are conditionally independent given X_1 ; the corresponding conditional density is $f(z | X_1) = (2k-2)z^{2k-3}$. In particular, for all $X_1 \in \mathbb{I}$, the conditional distribution and density of Z satisfy $F(z | X_1) = z^{2k-2}$ and $f(z | X_1) = (2k-2)z^{2k-3}$ for $0 \leq z \leq (2k-2)r$. Putting the pieces together, for $X_1 \in \mathbb{I}$,

$$\begin{aligned} & \mathbf{E}\left(\mathbf{1}_{[0, (2k-2)r]}(Z) e^{-n\alpha_2(X_1, X_{j^*})G(t)} | X_1\right) \\ &= \mathbf{E}\left(\mathbf{1}_{[0, 2r]}(Z) e^{-n\alpha_2(X_1, X_{j^*})G(t)} | X_1\right) + \mathbf{E}\left(\mathbf{1}_{(2r, (2k-2)r]}(Z) e^{-n\alpha_2(X_1, X_{j^*})G(t)} | X_1\right) \\ &\leq e^{-nr^2 G(t)} \int_0^{2r} (2k-2)z^{2k-3} e^{-nrzG(t)/\pi} dz + e^{-2nr^2 G(t)} \mathbf{P}\{2r < Z \leq (2k-2)r | X_1\} \\ &\leq (2k-2)e^{-nr^2 G(t)} \int_0^\infty z^{2k-3} e^{-nrzG(t)/\pi} dz + e^{-2nr^2 G(t)} \mathbf{P}\{Z \leq (2k-2)r | X_1\} \\ &= \pi^{2k-2} (2k-2)! \frac{r^{2k-2} e^{-nr^2 G(t)}}{(nr^2 G(t))^{2k-2}} + (2k-2)^{2k-2} r^{2k-2} e^{-2nr^2 G(t)} \\ &= \mathcal{O}\left(\frac{r^{2k-2}}{n \log^{2k-2} n} + \frac{r^{2k-2}}{n^2}\right) = \mathcal{O}\left(\frac{r^{2k-2}}{n \log^{2k-2} n}\right) \end{aligned}$$

where the order bounds are again uniform in X_1 . As $\mathbf{E}(1_{\mathbb{I}}(X_1)) = \mathbf{P}\{|X_1| \leq 1 - (2k-1)r\} = [1 - (2k-1)r]^2 = 1 + \mathcal{O}(r)$, substitution in (19) yields

$$K_{\text{interior}} = \mathcal{O}\left(\frac{r^{2k-2}}{n \log^{2k-2} n}\right) = \mathfrak{o}\left(\frac{1}{n^k}\right) \quad (20)$$

which is sub-dominant, if barely, compared to the non-overlap contribution $J_{\text{non-overlap}} \sim \lambda^k/n^k$ asymptotically as $n \rightarrow \infty$.

The boundary overlap contribution: As was the case for a single vertex, the calculations in the near-boundary are delicate and a careful case-by-case analysis is unavoidable. Write $\mathbf{1}_{[0, (2k-2)r]}(Z) = \mathbf{1}_{[0, 2r]}(Z) + \mathbf{1}_{(2r, (2k-2)r]}(Z)$ so that the expression for K_{boundary} in (19) can be written as the sum of two terms, one for *proximate* $Z \leq 2r$ when the visibility region of X_1 overlaps with that of each of X_2 through X_k and the other for *well-separated* $Z > 2r$ when

the two points X_1 and X_{j^*} are not adjacent in the overlap graph. We begin by disposing of the latter case first.

Well-separated Z: If $Z > 2r$ then $a_2(X_1, X_{j^*}) = a_1(X_1) + a_1(X_{j^*})$ as the visibility regions of X_1 and X_{j^*} do not overlap (even though there is a chain of overlaps connecting them in the overlap graph). The lower bound for a_1 in (8) shows then that $a_2(X_1, X_{j^*}) \geq r^2 - \frac{2}{\pi}r^3$ for all sufficiently large n while, as seen above, $\mathbf{P}\{2r < Z \leq (2k-2)r \mid X_1\} \leq [(2k-2)r]^{2(k-1)}$ and $\mathbf{E}(1_{\mathbb{S} \setminus \mathbb{I}}(X_1)) = 1 - \mathbf{P}\{|X_1| \leq 1 - (2k-1)r\} \leq (4k-2)r$. We hence obtain the asymptotic estimate

$$\begin{aligned} & \mathbf{E}\left[1_{\mathbb{S} \setminus \mathbb{I}}(X_1) \mathbf{E}(1_{(2r, (2k-2)r]}(Z) e^{-na_2(X_1, X_{j^*})G(t)} \mid X_1)\right] \\ & \leq (4k-2)(2k-2)^{2k-2} r^{2k-1} e^{-nr^2 G(t) + 2nr^3 G(t)/\pi} \\ & = \mathcal{O}\left(\frac{r^{2k-1}}{n}\right) = \mathfrak{o}\left(\frac{\log^{2k-1} n}{n^{k+1/2}}\right) = \mathfrak{o}\left(\frac{1}{n^k}\right) \end{aligned} \quad (21)$$

which, like the interior overlap contribution, is sub-dominant.

Proximate Z: We are left with the principal boundary overlap contributions arising from the regime $X_i \in \mathbb{S} \setminus \mathbb{I}$ and $Z \leq 2r$. As X_1 varies over the boundary $\mathbb{S} \setminus \mathbb{I}$, three regions may be identified: (i) the *very-near-boundary*, $1 - (2k-1)r < |X_1| \leq 1 - r$, when the disc of radius r centred at X_1 is completely contained within the unit disc; (ii) the *near-boundary*, $1 - r < |X_1| \leq \sqrt{1-r^2}$, as seen for a single vertex when part of the disc $\mathbb{D}(r; X_1)$ is lost to the visibility region due to intersection with the boundary; and (iii) the *far-boundary*, $\sqrt{1-r^2} < |X_1| \leq 1$, also as seen in the analysis for a single vertex when the area of the visibility region of X_1 is approximately $\frac{1}{2}\pi r^2$. Accordingly, write

$$1_{\mathbb{S} \setminus \mathbb{I}}(X_1) = 1_{(1-(2k-1)r, 1-r]}(|X_1|) + 1_{(1-r, \sqrt{1-r^2}]}(|X_1|) + 1_{(\sqrt{1-r^2}, 1]}(|X_1|)$$

and partition the range of X_1 to obtain

$$\mathbf{E}\left[1_{\mathbb{S} \setminus \mathbb{I}}(X_1) \mathbf{E}(1_{[0, 2r]}(Z) e^{-na_2(X_1, X_{j^*})G(t)} \mid X_1)\right] = B_{\text{boundary}}^{(i)} + B_{\text{boundary}}^{(ii)} + B_{\text{boundary}}^{(iii)} \quad (22)$$

where $B_{\text{boundary}}^{(i)}$ is the contribution from the very-near-boundary, $B_{\text{boundary}}^{(ii)}$ is the contribution from the near-boundary, and $B_{\text{boundary}}^{(iii)}$ is the contribution from the far-boundary.

Before proceeding further it will be useful to make two key observations at this point that will help to substantially simplify the calculations.

KEY OBSERVATION 1: *The conditional density of Z given X_1 has the uniform envelope $f(z \mid X_1) \leq (2k-2)z^{2k-3}$ for all $z \geq 0$. Indeed, for any $i \neq 1$, the conditional distribution of $|X_i - X_1|$ given X_1 is bounded by*

$$\mathbf{P}\{|X_i - X_1| \leq z \mid X_1\} = \frac{1}{\pi} \int_{\mathbb{D}(z; X_1) \cap \mathbb{S}} dx \leq \frac{1}{\pi} \int_{\mathbb{D}(z; X_1)} dx = z^2$$

for all $z \geq 0$ and it follows similarly that, for any $\epsilon > 0$,

$$\begin{aligned} \mathbf{P}\{z < |X_i - X_1| \leq z + \epsilon \mid X_1\} &= \frac{1}{\pi} \int_{\mathbb{D}(z+\epsilon; X_1) \setminus \mathbb{D}(z; X_1) \cap \mathbb{S}} dx \\ &\leq \frac{1}{\pi} \int_{\mathbb{D}(z+\epsilon; X_1) \setminus \mathbb{D}(z; X_1)} dx = (z + \epsilon)^2 - z^2 = 2z\epsilon + \epsilon^2 \end{aligned}$$

as the intersection with the unit circle of the annulus of width ϵ at the boundary of the circle of radius z centred at X_1 has area certainly no larger than that of the annulus itself. For convenience introduce the notational shorthand $F_2 = \mathbf{P}\{|X_i - X_1| \leq z\}$ and $\Delta F_2 = \mathbf{P}\{z < |X_i - X_1| \leq z + \epsilon \mid X_1\}$. As the event $\{z < Z \leq z + \epsilon\}$ occurs if, and only if, for some $j \geq 1$, exactly j of the X_i ($2 \leq i \leq k$) satisfy $z < |X_i - X_1| \leq z + \epsilon$ with the remaining $k - 1 - j$ of the X_i satisfying $|X_i - X_j| \leq z$ it follows that

$$\begin{aligned} \frac{1}{\epsilon} [F(z + \epsilon \mid X_1) - F(z \mid X_1)] &= \frac{1}{\epsilon} \mathbf{P}\{z < Z \leq z + \epsilon \mid X_1\} = \frac{1}{\epsilon} \sum_{j=1}^{k-1} \binom{k-1}{j} F_2^{k-1-j} [\Delta F_2]^j \\ &\leq \frac{1}{\epsilon} \sum_{j=1}^{k-1} \binom{k-1}{j} z^{2k-2-2j} (2z\epsilon + \epsilon^2)^j = \sum_{j=1}^{k-1} \binom{k-1}{j} z^{2k-2-2j} \epsilon^{j-1} (2z + \epsilon)^j. \end{aligned}$$

Allowing ϵ to tend to zero on both sides of the bound we obtain $f(z \mid X_1) \leq (2k - 2)z^{2k-3}$ as claimed.

KEY OBSERVATION 2: For given X_1 and Z , $a_2(X_1, X_{j^*})$ attains its minimum value when X_{j^*} is situated as closely as possible to the periphery of the unit disc. In particular, if $Z \leq 1 - |X_1|$ this is occasioned when X_{j^*} lies on the ray from the origin through the point X_1 and athwart X_1 and the circumference of the unit circle. And if $Z > 1 - |X_1|$ this is occasioned when X_{j^*} is one of the two points on the circumference of the unit circle at distance Z from X_1 . The validity of the observation may be seen as a consequence of the convexity of the circle whence $\mathbb{D}(r; X_{j^*}) \setminus \mathbb{D}(r; X_1)$ has its minimum area of overlap with the unit disc when X_{j^*} is situate on the point(s) on the circumference of the circle of radius Z centred at X_1 which is closest to the periphery of the unit disc. This observation is key as it allows us to repeatedly leverage our analysis for a single vertex.

The very-near-boundary: $1 - (2k - 1)r < |X_1| \leq 1 - r$. The simplest bounds suffice here. It is trivial that $A_2(X_1, X_{j^*}) \geq A_1(X_1) = \pi r^2$ so that $a_2(X_1, X_{j^*}) \geq r^2$. We hence obtain

$$\begin{aligned} B_{\text{boundary}}^{(i)} &\leq e^{-nr^2 G(t)} \mathbf{E} [1_{(1-(2k-1)r, 1-r]}(|X_1|) \mathbf{P}\{Z \leq 2r \mid X_1\}] \\ &\leq e^{-nr^2 G(t)} (4r^2)^{k-1} \mathbf{P}\{1 - (2k - 1)r < |X_1| \leq 1 - r\} \\ &= e^{-nr^2 G(t)} 4^{k-1} r^{2k-2} [(1 - r)^2 - (1 - (2k - 1)r)^2] \\ &\leq 4^k (k - 1) r^{2k-1} e^{-nr^2 G(t)} = \mathcal{O}\left(\frac{r^{2k-1}}{n}\right) = \mathcal{o}\left(\frac{\log^{2k-1} n}{n^{k+1/2}}\right) = \mathcal{o}\left(\frac{1}{n^k}\right) \end{aligned} \quad (23)$$

which is easily sub-dominant with respect to the main contribution from the interior.

The near-boundary: $1 - r < |X_1| \leq \sqrt{1 - r^2}$. As in the case of a single vertex, the situation is most delicate here and requires careful estimates. As Z varies from 0 to $2r$ two regions may be identified: (i) $0 \leq Z \leq 1 - |X_1|$ where the smallest value of $a_2(X_1, X_{j^*})$ occurs when X_{j^*} lies on the ray outward from the origin through the point X_1 , and (ii) $1 - |X_1| < Z \leq 2r$ when the smallest value of $a_2(X_1, X_{j^*})$ occurs when X_{j^*} is on the circumference of the unit circle at a distance Z from X_1 . The key to the analysis of both cases is identifying suitable bounds for $a_2(X_1, X_{j^*})$ explicitly as functions of $1 - |X_1|$ and Z .

(i) X_{j^*} is colinear with X_1 and the origin. In the worst case X_{j^*} is pinched into the narrow region between X_1 and the circumference of the unit disc and the worst-case area of the conjoined visibility region of X_1 and X_{j^*} will in consequence not be much larger than that of X_1 alone. But this is sufficient as we see next.

Leveraging our results for a single vertex we obtain

$$a_2(X_1, X_{j^*}) \geq a_1(X_1) \geq \frac{1}{2}r^2 + \frac{1}{\pi}r(1 - |X_1|)$$

by an appeal to (7). Consequently,

$$\begin{aligned} & \mathbf{E}\left[\mathbf{1}_{(1-r, \sqrt{1-r^2}]}(|X_1|) \mathbf{E}(1_{[0, 1-|X_1|]}(Z) e^{-na_2(X_1, X_{j^*})G(t)} \mid X_1)\right] \\ & \stackrel{\text{(vii)}}{\leq} 2(2k-2)e^{-nr^2G(t)/2} \int_{1-r}^{\sqrt{1-r^2}} d\rho \rho e^{-nr(1-\rho)G(t)/\pi} \int_0^{1-\rho} dz z^{2k-3} \\ & \stackrel{\text{(viii)}}{\leq} 2e^{-nr^2G(t)/2} \int_{1-r}^{\sqrt{1-r^2}} (1-\rho)^{2k-2} e^{-nr(1-\rho)G(t)/\pi} d\rho \\ & \stackrel{\text{(ix)}}{=} \frac{2\pi^{2k-1} e^{-nr^2G(t)/2}}{(nrG(t))^{2k-1}} \int_{nrG(t)(1-\sqrt{1-r^2})/\pi}^{nr^2G(t)/\pi} u^{2k-2} e^{-u} du \\ & \leq \frac{2\pi^{2k-1} e^{-nr^2G(t)/2}}{(nrG(t))^{2k-1}} \int_0^\infty u^{2k-2} e^{-u} du \\ & = \frac{2\pi^{2k-1} (2k-2)! r^{2k-1} e^{-nr^2G(t)/2}}{(nr^2G(t))^{2k-1}} = \mathcal{O}\left(\frac{r^{2k-1}}{\sqrt{n} \log^{2k-1} n}\right) = o\left(\frac{1}{n^k}\right) \quad (24) \end{aligned}$$

where (vii) follows from the key observation that the conditional density of Z has an envelope, in (viii) we use the fact that $\rho \leq \sqrt{1-r^2} < 1$ inside the integral, and (ix) follows from the change of variable of integration to $u = nr(1-\rho)G(t)/\pi$.

(ii) X_{j^*} is on the periphery. The situation is somewhat more complex here as, even in the worst-case, X_{j^*} situated on the circumference of the unit disc starts contributing more significantly to the conjoined region of visibility. Two cartoon figures illustrating this situation are shown in Figure 4. An arc of the circumference of the unit disc is shown passing

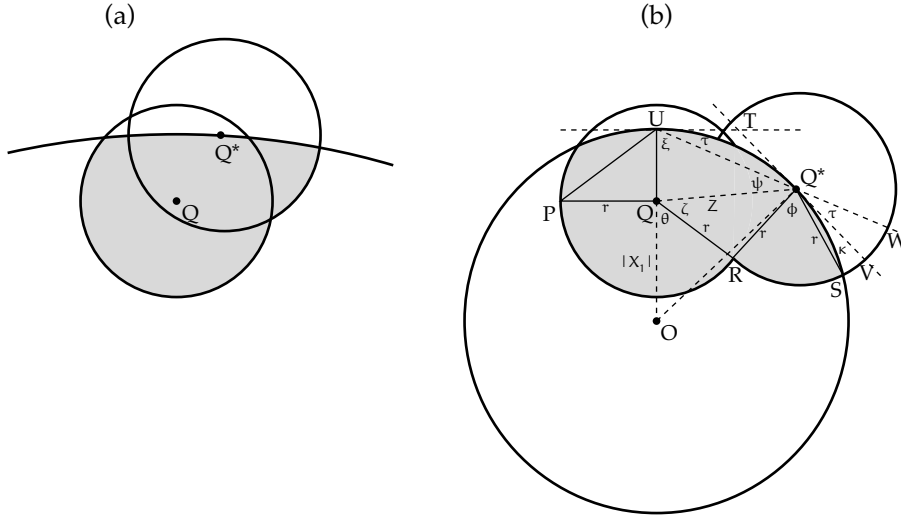


Figure 4: The near-boundary regime $1-r < |X_1| \leq \sqrt{1-r^2}$ for proximate Z satisfying $1-|X_1| < Z \leq 2r$. The point X_1 is situated at Q with X_{j^*} at Q^* on the periphery of the sensor field. The conjoined region of visibility is shown shaded.

through X_{j^*} situated at the point Q^* in Figure 4(a). On the scale of the radius r of the region of visibility, the intersection of the circumference of the unit disc with the circles of radius r at Q and Q^* is almost a straight line as shown in (a). In order to make the critical region more visible the curvature of the sensor field vis à vis the regions of visibility has been much exaggerated in Figure 4(b) where X_1 is situated at point Q and X_{j^*} at a distance $Z > 1 - |X_1|$ from X_1 is located on the circumference of the sensor field at point Q^* . We take our notation from this figure.

The right-angle triangle PQU whose base PQ has length r and height QU has length $1 - |X_1|$, the sector PQR of angle $\pi/2 + \theta$ of the circle of radius r at Q , and the sector RQ^*S of angle ϕ of the circle of radius r at Q^* are non-overlapping and contained wholly within the conjoined visibility region $\mathbb{V}(X_1) \cup \mathbb{V}(X_{j^*})$. It follows that

$$A_2(X_1, X_{j^*}) \geq \frac{1}{2}r(1 - |X_1|) + \frac{1}{2}r^2\left(\frac{\pi}{2} + \theta\right) + \frac{1}{2}r^2\phi.$$

Elementary calculations now serve to determine the various angles of interest.

1. Let Z' denotes the length of the line segment UQ^* . As two sides of a triangle are larger than the third, a consideration of triangle QUQ^* shows that $Z' \leq Z + (1 - |X_1|) \leq 3r$ as $Z \leq 2r$ and $1 - |X_1| < r$.
2. As UOQ^* is an isosceles triangle with sides of length 1 and base of length Z' , we have $\xi = \angle OUQ^* = \arccos\left(\frac{Z'}{2}\right) = \frac{\pi}{2} - \arcsin\left(\frac{Z'}{2}\right)$.
3. As UT is the tangent line at U , $\tau = \angle TUQ^* = \frac{\pi}{2} - \xi = \arcsin\left(\frac{Z'}{2}\right) \leq Z' \leq 3r$ for large enough n by virtue of the upper bound for the arcsine function from Lemma 1. With TQ^*V the tangent line at Q^* , note that τ may also be identified with $\angle VQ^*W$.
4. As QRQ^* is an isosceles triangle with sides r and base Z , we have $\zeta = \angle RQ^*Q = \angle RQ^*Q = \frac{\pi}{2} - \arcsin\left(\frac{Z}{2r}\right) \leq \frac{\pi}{2} - \frac{Z}{2r}$, by virtue of the lower bound for the arcsine function this time, again from Lemma 1.
5. With $\kappa = \angle SQ^*V$, the development leading up to (8) in the analysis of the far-boundary for a single vertex shows that $r^2\left(\frac{\pi}{2} - \kappa\right) \geq \frac{\pi}{2}r^2 - r^3$ so that $\kappa \leq r$.
6. With $\psi = \angle QQ^*U$, it follows that $\phi = \pi - \psi - \zeta - \kappa - \tau \geq \frac{\pi}{2} - \psi + \frac{Z}{2r} - 4r$.
7. And finally, an examination of the exterior angle of the triangle UQQ^* shows that $\theta + \zeta = \xi + \psi$ so that $\theta = \frac{\pi}{2} - \tau + \psi - \zeta \geq \psi + \frac{Z}{2r} - 3r$.

Proceeding with bounding the area of the conjoined region of visibility, we have

$$A_2(X_1, X_{j^*}) \geq \frac{1}{2}r(1 - |X_1|) + \frac{1}{2}r^2\left(\frac{\pi}{2} + \theta + \phi\right) \geq \frac{1}{2}\pi r^2 + \frac{1}{2}r(1 - |X_1|) + \frac{1}{2}rZ - \frac{7}{2}r^3,$$

and, in consequence,

$$a_2(X_1, X_{j^*}) \geq \frac{1}{2}r^2 + \frac{1}{2\pi}r(1 - |X_1|) + \frac{1}{2\pi}rZ - \frac{7}{2\pi}r^3.$$

Again exploiting the fact that the conditional density of Z has a uniform envelope, we obtain

$$\begin{aligned} & \mathbf{E}\left[1_{(1-r, \sqrt{1-r^2}]}\left(|X_1|\right) \mathbf{E}\left(1_{(1-|X_1|, 2r]}(Z) e^{-na_2(X_1, X_{j^*})G(t)} \mid X_1\right)\right] \\ & \leq 2(2k-2)e^{-\frac{1}{2}nr^2G(t) + \frac{7}{2\pi}nr^3G(t)} \int_{1-r}^{\sqrt{1-r^2}} d\rho \rho e^{-nr(1-\rho)G(t)/2\pi} \int_{1-\rho}^{2r} dz z^{2k-3} e^{-nrzG(t)/2\pi}. \end{aligned}$$

Finish off by bounding the inner integral first,

$$\int_{1-\rho}^{2r} z^{2k-3} e^{-nrzG(t)/2\pi} dz \leq \int_0^\infty z^{2k-3} e^{-nrzG(t)/2\pi} dz = \frac{(2k-3)!(2\pi)^{2k-2}}{(nrG(t))^{2k-2}},$$

then the outer integral,

$$\begin{aligned} \int_{1-r}^{\sqrt{1-r^2}} 2\rho e^{-nr(1-\rho)G(t)/2\pi} d\rho &\leq 2 \int_{1-\sqrt{1-r^2}}^r e^{-nr u G(t)/2\pi} du \\ &\leq 2 \int_0^\infty e^{-nr u G(t)/2\pi} du = \frac{4\pi}{nrG(t)}, \end{aligned}$$

via the change of variable of integration $u \leftarrow 1 - \rho$, to finally obtain the bound

$$\begin{aligned} &\mathbf{E} \left[\mathbf{1}_{(1-r, \sqrt{1-r^2}]}(|X_1|) \mathbf{E} \left(\mathbf{1}_{(1-|X_1|, 2r]}(Z) e^{-na_2(X_1, X_{1,*})G(t)} \mid X_1 \right) \right] \\ &\leq 2^{2k} \pi^{2k-1} (2k-2)! \frac{r^{2k-1} e^{-\frac{1}{2}nr^2G(t) + \frac{7}{2\pi}nr^3G(t)}}{(nr^2G(t))^{2k-1}} = \mathcal{O} \left(\frac{r^{2k-1}}{\sqrt{n} \log^{2k-1} n} \right) = \mathfrak{o} \left(\frac{1}{n^k} \right). \end{aligned} \quad (25)$$

Mop up by putting (24) and (25) together to get

$$\begin{aligned} B_{\text{boundary}}^{(ii)} &= \mathbf{E} \left[\mathbf{1}_{(1-r, \sqrt{1-r^2}]}(|X_1|) \mathbf{E} \left(\mathbf{1}_{[0, 2r]}(Z) e^{-na_2(X_1, X_{1,*})G(t)} \mid X_1 \right) \right] \\ &= \mathcal{O} \left(\frac{r^{2k-1}}{\sqrt{n} \log^{2k-1} n} \right) = \mathfrak{o} \left(\frac{1}{n^k} \right) \end{aligned} \quad (26)$$

which is again of the requisite asymptotic order, though barely so for the given rate of $r = r_n$.

The far-boundary: $\sqrt{1-r^2} < |X_1| \leq 1$. Borrowing again from the analysis for a single vertex, we have from (8) that $a_2(X_1, X_{1,*}) \geq a_1(X_1) \geq \frac{1}{2}r^2 - \frac{1}{\pi}r^3$ for sufficiently large n . It follows that

$$\begin{aligned} B_{\text{boundary}}^{(iii)} &= \mathbf{E} \left[\mathbf{1}_{(\sqrt{1-r^2}, 1]}(|X_1|) \mathbf{E} \left(\mathbf{1}_{[0, 2r]}(Z) e^{-na_2(X_1, X_{1,*})G(t)} \mid X_1 \right) \right] \\ &\leq e^{-\frac{1}{2}nr^2G(t) + \frac{1}{\pi}nr^3G(t)} \mathbf{E} \left[\mathbf{1}_{(\sqrt{1-r^2}, 1]}(|X_1|) \mathbf{P}\{Z \leq 2r \mid X_1\} \right] \\ &\leq e^{-\frac{1}{2}nr^2G(t) + \frac{1}{\pi}nr^3G(t)} (4r^2)^{k-1} \mathbf{P}\{\sqrt{1-r^2} < |X_1| \leq 1\} \\ &\leq e^{-\frac{1}{2}nr^2G(t) + \frac{1}{\pi}nr^3G(t)} (4r^2)^{k-1} [1 - (1-r^2)] \\ &= \mathcal{O} \left(\frac{r^{2k}}{\sqrt{n}} \right) = \mathfrak{o} \left(\frac{\log^{2k} n}{n^{k+1/2}} \right) = \mathfrak{o} \left(\frac{1}{n^k} \right) \end{aligned} \quad (27)$$

which is also asymptotically sub-dominant.

Finale. We can now trace our way back to the starting point. Stitching the boundary contributions for proximate Z together in (22) we have from (23), (26), and (27) that

$$\mathbf{E} \left[\mathbf{1}_{\mathbb{S} \setminus \mathbb{I}}(X_1) \mathbf{E} \left(\mathbf{1}_{[0, 2r]}(Z) e^{-na_2(X_1, X_{1,*})G(t)} \mid X_1 \right) \right] = \mathfrak{o}(n^{-k})$$

which together with the estimate (21) when Z is well-separated implies that $K_{\text{boundary}} = \mathfrak{o}(n^{-k})$ in (19), which, in turn, in conjunction with the corresponding estimate (20) for K_{interior} yields $K(n) = K_{\text{interior}} + K_{\text{boundary}} = \mathfrak{o}(n^{-k})$, which then implies in (18) that

$$\mathbf{E} \left[\mathbf{1}_{\mathbb{C}_k}(X_1, \dots, X_k) e^{-na_k(X_1, \dots, X_k)G(t)} \right] = \mathfrak{o}(n^{-k}). \quad (28)$$

At long last the weariest river winds its way safely to sea. The last estimate returns us finally to (17) and (15) from which we conclude that $J_k = o(n^{-k})$ and the contribution due to connected overlap graphs is asymptotically sub-dominant.

Overlapping regions of visibility, conclusion. Return to the system of equations (14, 14') reproduced here for convenience. The contribution from all overlap graphs $\mathcal{F} \neq \mathcal{F}_*$ to the probability of the event that vertices X_1 through X_k are all isolated by time t is

$$J_{\text{overlap}} = \sum_{\gamma=1}^{k-1} \sum_{\substack{k_1 \geq \dots \geq k_\gamma \geq 1 \\ k_1 + \dots + k_\gamma = k}} J_{k_1, \dots, k_\gamma}$$

where J_{k_1, \dots, k_γ} is the total contribution from all overlap graphs $\mathcal{F}_{k_1, \dots, k_\gamma}$ with exactly γ components of sizes k_1, \dots, k_γ and is given by

$$J_{k_1, \dots, k_\gamma} = \sum_{\mathcal{F}_{k_1, \dots, k_\gamma}} \mathbf{E} [1_{\mathcal{C}(\mathcal{F}_{k_1, \dots, k_\gamma})}(X_1, \dots, X_k) \mathbf{P}({}^0L_{1, \dots, k}(t) | X_1, \dots, X_k)].$$

Some algebraic simplification in the expression for J_{k_1, \dots, k_γ} can be achieved by observing that as the points X_1, \dots, X_n are generated by independent sampling from the uniform distribution on the unit disc, it follows by symmetry that any two overlap graphs $\mathcal{F}_{k_1, \dots, k_\gamma}$ and $\mathcal{F}'_{k_1, \dots, k_\gamma}$ that differ only in a permutation of the vertices will contribute exactly the same amount to the sum for J_{k_1, \dots, k_γ} . As there are exactly $k!/(k_1! \dots k_\gamma!)$ allocations of the vertices from X_1 to X_k into γ cells with respective occupancies k_1, \dots, k_γ , it follows that

$$J_{k_1, \dots, k_\gamma} = \frac{k!}{k_1! \dots k_\gamma!} \sum'_{\mathcal{F}_{k_1, \dots, k_\gamma}} \mathbf{E} [1_{\mathcal{C}(\mathcal{F}_{k_1, \dots, k_\gamma})}(X_1, \dots, X_k) \mathbf{P}({}^0L_{1, \dots, k}(t) | X_1, \dots, X_k)]$$

where the sum \sum' is now restricted to overlap graphs $\mathcal{F}_{k_1, \dots, k_\gamma}$ for which the first component consists of the first k_1 vertices $\{X_1, \dots, X_{k_1}\}$, the second component consists of the next k_2 vertices $\{X_{k_1+1}, \dots, X_{k_1+k_2}\}$, and so on, with the γ th component consisting of the final k_γ vertices $\{X_{k-k_\gamma+1}, \dots, X_k\}$. As in the case of the connected overlap graphs we now proceed to further consolidate these graphs.

Write $\mathcal{C}_{k_1, \dots, k_\gamma}$ for the subset of k -tuples (X_1, \dots, X_k) for which the corresponding overlap graph is divided into γ components with the first component comprised of the vertices $\{X_1, \dots, X_{k_1}\}$, the second component of the vertices $\{X_{k_1+1}, \dots, X_{k_1+k_2}\}$, and so on, with the γ th component consisting of the vertices $\{X_{k-k_\gamma+1}, \dots, X_k\}$. It is then clear that the sum $\sum'_{\mathcal{F}_{k_1, \dots, k_\gamma}} 1_{\mathcal{C}(\mathcal{F}_{k_1, \dots, k_\gamma})}(X_1, \dots, X_k)$ is itself the indicator for the set $\mathcal{C}_{k_1, \dots, k_\gamma}$ and consequently

$$J_{k_1, \dots, k_\gamma} = \frac{k!}{k_1! \dots k_\gamma!} \mathbf{E} [1_{\mathcal{C}_{k_1, \dots, k_\gamma}}(X_1, \dots, X_k) \mathbf{P}({}^0L_{1, \dots, k}(t) | X_1, \dots, X_k)].$$

One final piece of notation to help compact expressions: for $j = 1, \dots, \gamma$, introduce the nonce notation $x^{(j)} = (x_{k_1 + \dots + k_{j-1} + 1}, \dots, x_{k_1 + \dots + k_j})$ to indicate the j th subsequence of length k_j and, mirroring the notation introduced for connected overlap graphs, let \mathcal{C}_{k_j} denote the set of k_j -tuples $x^{(j)}$ in \mathbb{S}^{k_j} for which the overlap graph $\mathcal{H}_{k_j}(x^{(j)})$ is connected. We may now range through the k -tuples (x_1, \dots, x_k) comprising the set $\mathcal{C}_{k_1, \dots, k_\gamma}$ recursively as follows:

BASE: The k_1 -tuple $x^{(1)}$ is allowed to range over the subset $\mathcal{C}_{k_1}^{(1)} = \mathcal{C}_{k_1}$ of \mathbb{S}^{k_1} for which the overlap graph $\mathcal{H}_{k_1}(x^{(1)})$ is connected.

RECURRENCE: As j ranges from 2 to γ , for every selection of $x_1, \dots, x_{k_1+\dots+k_{j-1}}$, the k_j -tuple $x^{(j)}$ is allowed to range over the subset $\mathbb{C}_{k_j}^{(j)} = \mathbb{C}_{k_j} \setminus \left(\bigcup_{i=1}^{k_1+\dots+k_{j-1}} \mathbb{O}(x_i)\right)^{k_j}$ of \mathbb{S}^{k_j} for which the overlap graph $\mathcal{H}_{k_j}(x^{(j)})$ is connected while avoiding the overlap regions of the points $x_1, \dots, x_{k_1+\dots+k_{j-1}}$.

Write $dx^{(j)} = dx_{k_1+\dots+k_{j-1}+1} \cdots dx_{k_1+\dots+k_j}$ in the natural extension of the notation to the differential. It then follows that

$$J_{k_1, \dots, k_\gamma} = \frac{k!}{k_1! \cdots k_\gamma!} \frac{1}{\pi^k} \int_{\mathbb{C}_{k_1}^{(1)}} dx^{(1)} \int_{\mathbb{C}_{k_2}^{(2)}} dx^{(2)} \cdots \int_{\mathbb{C}_{k_\gamma}^{(\gamma)}} dx^{(\gamma)} \mathbf{P}({}^0L_{1, \dots, k}(t) \mid X_1 = x_1, \dots, X_k = x_k)$$

Now arguing as in (16), we obtain the bound

$$\mathbf{P}({}^0L_{1, \dots, k}(t) \mid X_1 = x_1, \dots, X_k = x_k) \leq \left[1 + \mathcal{O}\left(\frac{\log^2 n}{n}\right)\right] e^{-n a_k(x_1, \dots, x_k) G(t)}$$

where, for each k -tuple (x_1, \dots, x_k) in $\mathbb{C}_{k_1, \dots, k_\gamma}$, we have

$$a_k(x_1, \dots, x_k) = a_{k_1}(x^{(1)}) + a_{k_2}(x^{(2)}) + a_{k_3}(x^{(3)}) + \cdots + a_{k_\gamma}(x^{(\gamma)})$$

as the visibility regions across components do not overlap. It then follows that

$$J_{k_1, \dots, k_\gamma} \leq \left[1 + \mathcal{O}\left(\frac{\log^2 n}{n}\right)\right] \frac{k!}{k_1! \cdots k_\gamma!} \frac{1}{\pi^{k_1}} \int_{\mathbb{C}_{k_1}^{(1)}} dx^{(1)} e^{-n a_{k_1}(x^{(1)}) G(t)} \times \frac{1}{\pi^{k_2}} \int_{\mathbb{C}_{k_2}^{(2)}} dx^{(2)} e^{-n a_{k_2}(x^{(2)}) G(t)} \cdots \frac{1}{\pi^{k_\gamma}} \int_{\mathbb{C}_{k_\gamma}^{(\gamma)}} dx^{(\gamma)} e^{-n a_{k_\gamma}(x^{(\gamma)}) G(t)}. \quad (29)$$

A typical nested integral on the right-hand side is of the form

$$\frac{1}{\pi^{k_j}} \int_{\mathbb{C}_{k_j}^{(j)}} dx^{(j)} e^{-n a_{k_j}(x^{(j)}) G(t)} = \mathbf{E} \left[\mathbf{1}_{\mathbb{C}_{k_j}^{(j)}}(X^{(j)}) e^{-n a_{k_j}(X^{(j)}) G(t)} \mid X_1 = x_1, \dots, X_{k_1+\dots+k_{j-1}} = x_{k_1+\dots+k_{j-1}} \right] \quad (30)$$

and exhibits one of two distinct behaviours depending on the value of k_j . If $k_j = 1$ (that is the j th component consists of a singleton point) then as per our earlier calculations in (12) the integral differs from λ/n only by a multiplicative term $1 + o(1)$ as $\mathbb{C}_{k_j}^{(j)}$ differs from $\mathbb{S}^{k_j} = \mathbb{S}$ only in a region $\bigcup_{i=1}^{k_1+\dots+k_{j-1}} \mathbb{O}(x_i)$ whose area is of order $\mathcal{O}(r^2)$. If $k_j \geq 2$ on the other hand then the integral is bounded above by

$$\mathbf{E} \left[\mathbf{1}_{\mathbb{C}_{k_j}}(X^{(j)}) e^{-n a_{k_j}(X^{(j)}) G(t)} \right]$$

as $\mathbb{C}_{k_j}^{(j)} \subset \mathbb{C}_{k_j}$ and the set \mathbb{C}_{k_j} is independent of $X_1, \dots, X_{k_1+\dots+k_{j-1}}$. But the last equation differs only notationally in the replacement of k by k_j from the expectation on the right-hand side of the bound (17) for J_k . The results of our analysis for connected overlap graphs hence carries over *in toto* and, as per the estimate (28), the integral (30) is asymptotically $o(n^{-k_j})$.

Suppose now that there are exactly j components, say i_1, \dots, i_j , each of which consists of two or more vertices with the remaining $\gamma - j$ components being singletons. Bear in mind that $j \geq 1$ as $\gamma < k$ so that there is at least one non-singleton component. Clearly, also, $k_{i_1} + \dots + k_{i_j} = k - \gamma + j$. Each of the $\gamma - j$ singleton components contributes a multiplicative factor of $\frac{\lambda}{n}(1 + o(1))$ to the right-hand side of (29) so that the cumulative multiplicative contribution of the singleton components to the expression for J_{k_1, \dots, k_γ} is $\frac{\lambda^{\gamma-j}}{n^{\gamma-j}}(1 + o(1))$. On the other hand, the $j \geq 1$ non-singleton components contribute multiplicative factors of $o(n^{-k_{i_1}}), \dots, o(n^{-k_{i_j}})$, respectively, for a cumulative multiplicative factor of $o(n^{-(k_{i_1} + \dots + k_{i_j})})$. Putting both terms together we obtain the asymptotic estimate

$$J_{k_1, \dots, k_\gamma} = o\left(\frac{1}{n^{k_{i_1} + \dots + k_{i_j}}} \times \frac{1}{n^{\gamma-j}}\right) \quad (n \rightarrow \infty).$$

Thus each of the summands in the expression for J_{overlap} is $o(n^{-k})$ and as the sum ranges over only a bounded number of terms we conclude that $J_{\text{overlap}} = o(n^{-k})$ as well. Together with our hard-won estimate $J_{\text{non-overlap}} \sim \lambda^k/n^k$ in (13), this completes our evaluation of the system of equations (11).

Joint isolation probability. Returning finally to (10) we obtain $\mathbf{P}({}^0L_{1, \dots, k}(t)) = J_{\text{non-overlap}} + J_{\text{overlap}} = \frac{\lambda^k}{n^k}(1 + o(1)) + o(\frac{1}{n^k}) \sim \frac{\lambda^k}{n^k}$. It follows that, as claimed, for any fixed positive integer k and any collection of k distinct indices i_1, \dots, i_k , $\mathbf{P}({}^0L_{i_1, \dots, i_k}(t)) \sim \frac{\lambda^k}{n^k}$ as $n \rightarrow \infty$. Recall that our analysis for a single vertex revealed that $\mathbf{P}({}^0L_i(t)) = {}^0P(t) \sim \frac{\lambda}{n}$. Thus, for any group of k vertices we have shown that $\mathbf{P}({}^0L_{i_1}(t) \cap \dots \cap {}^0L_{i_k}(t)) \sim [{}^0P(t)]^k$ and we may paraphrase this succinctly, if somewhat imprecisely, by saying that the events ${}^0L_i(t)$ are weakly asymptotically independent.

3° A POISSON SIEVE. The stage is set for an application of Bonferroni's inequalities (Lemma 2). Let $S_k(n)$ denote the sum of all the probabilities of k -fold conjunctions of the events ${}^0L_i(t)$ ($1 \leq i \leq n$). As $n \rightarrow \infty$ we obtain

$$S_k(n) = \sum_{1 \leq i_1 < \dots < i_k \leq n} \mathbf{P}({}^0L_{i_1}(t) \cap \dots \cap {}^0L_{i_k}(t)) = \binom{n}{k} \mathbf{P}({}^0L_{1, \dots, k}(t)) \sim \binom{n}{k} \frac{\lambda^k}{n^k}.$$

Now $\binom{n}{k} = \frac{1}{k!} n(n-1) \dots (n-k+1) = \frac{n^k}{k!} [1 + O(\frac{1}{n})] \sim \frac{n^k}{k!}$ where, of course, k is fixed and n tends to infinity. It follows that, for every positive integer k , $S_k(n) \rightarrow \frac{\lambda^k}{k!}$ as $n \rightarrow \infty$. Hence, for every fixed K ,

$$\sum_{k=0}^K (-1)^k \binom{m+k}{m} S_{m+k}(n) \rightarrow \sum_{k=0}^K \frac{(-1)^k \lambda^{m+k}}{(m+k)!} \frac{(m+k)!}{m!k!} = \frac{\lambda^m}{m!} \sum_{k=0}^K \frac{(-\lambda)^k}{k!}$$

as $n \rightarrow \infty$. We recognise the truncated Taylor series for $e^{-\lambda}$ on the right-hand side. As the exponential series $e^x = \sum_{k=0}^{\infty} x^k/k!$ converges absolutely (and uniformly over every closed and bounded interval) it follows that for every $\epsilon > 0$ we can select $K = K(\epsilon)$ so that

$$\left| \sum_{k=0}^K \frac{(-\lambda)^k}{k!} - e^{-\lambda} \right| < \epsilon.$$

Let m be any nonnegative integer. Then the event $\{{}^0N(t) = m\}$ that there are exactly m isolated vertices at time t in the graph $\mathcal{G}_{n,r}$ occurs if, and only if, precisely m of the events

$\{ {}^0L_i(t), 1 \leq i \leq n \}$ occur. By Lemma 2, for every $\epsilon > 0$ we may select a sufficiently large value of K so that

$$\begin{aligned} (e^{-\lambda} - \epsilon) \frac{\lambda^m}{m!} &< \sum_{k=0}^{2K-1} (-1)^k \binom{m+k}{m} S_{m+k}(n) \leq \mathbf{P}\{ {}^0N(t) = m \} \\ &\leq \sum_{k=0}^{2K} (-1)^k \binom{m+k}{m} S_{m+k}(n) < (e^{-\lambda} + \epsilon) \frac{\lambda^m}{m!} \end{aligned}$$

with the book-end inequalities on either side holding for all sufficiently large n . As the tiny ϵ is arbitrary, it follows that $\mathbf{P}\{ {}^0N(t) = m \} \rightarrow e^{-\lambda} \lambda^m / m!$ as $n \rightarrow \infty$, as advertised. This completes the proof of the theorem for the case of isolated vertices $\ell = 0$ in the graph $\mathcal{G}_{n,r}$.

The proofs of the general result and the corollaries require only small adaptations to the framework of the proof for isolated vertices.

THE MAIN THEOREM: Recall that the disc $\mathbb{D}_i(\ell)$ is isolated at time t in $\mathcal{G}_{n,r}$ if the annulus $\mathbb{D}_i(\ell, \ell+r)$ contains no live vertices at time t . Adapt the earlier notation and write $A(X_i)$ for the area of the intersection of $\mathbb{D}_i(\ell, \ell+r)$ with the unit disc \mathbb{S} . Then $\alpha(X_i) = A(X_i)/\pi$ is the probability that a random vertex will lie in $\mathbb{D}_i(\ell, \ell+r) \cap \mathbb{S}$. Arguing as before, conditioned on X_i the probability that $\mathbb{D}_i(\ell)$ is isolated at time t in $\mathcal{G}_{n,r}$ is then $(1 - \alpha(X_i)G(t))^{n-1}$. Taking expectation gives us the unconditional probability of isolation of the disc of radius ℓ centred at the i th vertex

$${}^\ell p(t) = \mathbf{E}\{ (1 - \alpha(X_i)G(t))^{n-1} \} \quad (5')$$

which generalises the corresponding expression (5) for isolated vertices.

It is clear, as before, that $\alpha(X_i)$ depends only on $|X_i|$, the distance of X_i from the origin. If X_i lies in the interior of the unit disc with $|X_i| \leq 1 - \ell - r$ then $\alpha(X_i) = (\ell+r)^2 - \ell^2 = 2\ell r + r^2 \triangleq R^2$ with $\alpha(X_i)$ decreasing monotonically thereafter to a value close to $R^2/2$ as $|X_i|$ increases from $1 - \ell - r$ to 1; see Figure 5. Redefine the interior to mean the region $|X_i| \leq 1 - \ell - r$. The interior contribution to the expectation integral (5') is then asymptotic to $e^{-nR^2G(t)}$. Arguing as for an isolated vertex, the contribution of the boundary to ${}^\ell p(t)$ is sub-dominant so that ${}^\ell p(t) \sim e^{-nR^2G(t)} \sim \lambda/n$ under the conditions of the main theorem.

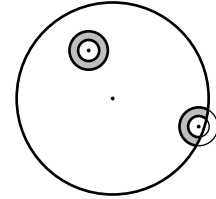


Figure 5: Visibility annuli.

The rest of the proof proceeds exactly as before with the systematic replacement of references to r in the proof for isolated vertices by $R = \sqrt{2\ell r + r^2}$. The steps in the proof remain unaltered with the geometry only slightly messier as annuli replace discs of visibility. We eschew the unedifying details.

COROLLARY 1: If we set $\ell_n = 0$ and $r_n = c_n$ in the main theorem we obtain $R_n = c_n$. The conditions (1) then specialise to (1') and the stated result follows.

COROLLARY 2: Recall that there is a lacuna of radius ℓ centred at vertex X_i at time t if there are no live vertices in (1) the annulus $\mathbb{D}_i(\ell, \ell+s)$, and (2) at least one of the disc $\mathbb{D}_i(\ell)$ and the annulus $\mathbb{D}_i(\ell, \ell+c)$. Temporarily write $Q_n = Q_n(\ell, s, c, t)$ for the probability that there is a lacuna of radius ℓ centred at a network vertex at time t . There are two cases possible depending on whether $s > c$ or $s \leq c$. We consider these in turn.

Suppose $s > c$. Clearly, if there are no live vertices in $\mathbb{D}_i(\ell, \ell+s)$ then there will certainly be no live vertices in $\mathbb{D}_i(\ell, \ell+c)$ so that condition (2) follows trivially if condition (1) holds. Consequently, there is a lacuna of radius ℓ centred at vertex X_i at time t if, and only

if, at time t there are no live vertices in $\mathbb{D}_i(\ell, \ell + s)$, or, equivalently, the disc $\mathbb{D}_i(\ell)$ is isolated in the graph $\mathcal{G}_{n,s}$. Arguing as in the main theorem for an isolated disc, it follows that

$$Q_n \sim e^{-n[(\ell+s)^2 - \ell^2]G(t)}. \quad (31)$$

when $s > c$.

Now consider the case $s \leq c$. There are two mutually exclusive cases depending on whether there are any live vertices in the disc $\mathbb{D}_i(\ell)$.

(i) Conditioned on the event that there are no live vertices in $\mathbb{D}_i(\ell)$ at time t , there will be a lacuna of radius ℓ centred at X_i at time t if, and only if, there are no live vertices in $\mathbb{D}_i(\ell, \ell + s)$ at that time. The probability that there are no live vertices in both $\mathbb{D}_i(\ell)$ and $\mathbb{D}_i(\ell, \ell + s)$ is equal to the probability that vertex X_i is extinguished as well as isolated in $\mathcal{G}_{n,\ell+s}$ and the line of argument leading to the main theorem shows that this is asymptotic to

$$(1 - G(t))e^{-n(\ell+s)^2G(t)} \quad (32)$$

as the extinction of the vertex X_i is independent of the extinction of other vertices.

(ii) Conditioned on the event that there exist live vertices in $\mathbb{D}_i(\ell)$ at time t , there will be a lacuna of radius ℓ centred at X_i at time t if, and only if, there are no live vertices in $\mathbb{D}_i(\ell, \ell + c)$ (as this event will also imply that there are no live vertices in $\mathbb{D}_i(\ell, \ell + s)$ when $s \leq c$), or, equivalently, disc $\mathbb{D}_i(\ell)$ is isolated in $\mathcal{G}_{n,c}$. Arguing as in (32), the probability that there are live vertices in the disc $\mathbb{D}_i(\ell)$ at time t is asymptotic to $1 - (1 - G(t))e^{-n\ell^2G(t)}$ and, likewise, following the line of the main theorem, the probability that $\mathbb{D}_i(\ell)$ is isolated in $\mathcal{G}_{n,c}$ at time t is asymptotic to $e^{-n[(\ell+c)^2 - \ell^2]G(t)}$. As vertex extinctions are independent, it follows that the probability that, at time t , the disc $\mathbb{D}_i(\ell)$ contains live vertices but is isolated in $\mathcal{G}_{n,c}$ is asymptotic to

$$e^{-n[(\ell+c)^2 - \ell^2]G(t)} \{1 - (1 - G(t))e^{-n\ell^2G(t)}\} = e^{-n[(\ell+c)^2 - \ell^2]G(t)} - (1 - G(t))e^{-n(\ell+c)^2G(t)}. \quad (33)$$

Combining the asymptotic estimates (32) and (33) we obtain

$$Q_n \sim e^{-n[(\ell+c)^2 - \ell^2]G(t)} + (1 - G(t)) \{e^{-n(\ell+s)^2G(t)} - e^{-n(\ell+c)^2G(t)}\} \quad (34)$$

when $s \leq c$.

The right-hand sides of (31) and (34) may be combined into the single expression $P_n = P_n(\ell, s, c, t)$ given by (2). Accordingly, we have shown that the probability that there is a lacuna of radius ℓ at any given network vertex at time t is given asymptotically by $Q_n \sim P_n \sim \lambda/n$ under the conditions of the corollary. The rest of the proof follows the steps of the proof for single vertex isolation. Following that line of argument, the probability that there are lacunae of radius ℓ at any k given network vertices at time t is asymptotic to $\lambda^k/k!$ and inclusion-exclusion completes the proof as before. Q.E.D.

6 Concluding Remarks

The phase transitions that are so characteristic of random graph phenomena make their appearance in this setting in the time to emergence of sensory lacunae. The Poisson laws that are the content of our main theorem provide a detailed picture of the situation at the critical time; these results provide explicit and fundamental tradeoffs between transmission power, vertex density, and network lifetime and suggest, as we saw in the examples of Section 3, how principled choices can be made to improve the lifetime of the network.

Several other questions are suggested in this framework. For instance, one may wish to track how network connectivity evolves as vertices are extinguished. In particular, one may wish to characterise when connectivity among vertex *survivors* first breaks down. In a concurrent paper we demonstrate that survivor connectivity also exhibits a phase transition at a critical time [13, 14].

The conditions under which our theorem operates are of course highly sanitised and several points of departure toward more complicated (and perhaps realistic) models are suggested. We discuss a few of these.

From circular to non-circular and irregular regions of deployment: A consideration of the proof of the main theorem shows that most of the effort was expended in showing that boundary and overlap effects are ultimately negligible in a certain domain. It should be clear from the analysis that the result, while presented for a circular sensor field, should carry through to other shapes as well; roughly speaking, all that is required is that the perimeter does not dominate the interior. Thus, “fat” or “blobby” shapes are in; “thin” or “squiggly” shapes are out. Penrose [16], for instance, considers random geometric graphs in the unit square. Our results translate into this setting with essentially no change barring a proper normalisation for area. One anticipates, for instance, that more generally the results will carry through to “fat” convex shapes though this question is open.

From hard-sphere communication and sensing models to soft, probabilistic models: The spherical 0–1 communication model in which two vertices can communicate error-free if they lie no further than their common communication radius apart is popular but does not correlate well with real-life instances of wireless networks. In practice the capability of two vertices to communicate depends on a variety of factors such as distance, antenna beam patterns, and the relative positions of the communicating vertices and interferers. In a more realistic model we may replace the hard-sphere model of communication by probabilistic models where the ability of two vertices to communicate with each other is modelled as a probability distribution parametrised by various factors such as antenna orientation, distance, and channel noise. The analysis segues smoothly into such situations though we reserve the details. Similar comments apply to the hard-sphere sensing model.

From independent battery lifetimes with a common parametrised distribution to topology- and protocol-dependent distributions: The assumption that battery lifetime distributions are independent and identically distributed appears to be the most unrealistic. The multihop nature of message transmissions in such settings suggests that battery lifetimes will be correlated. To complicate the picture further, dependencies in battery lifetimes are likely to be significantly impacted both by the network topology and the protocols used. Attempts at relaxing the independent lifetime assumption would be of significant interest though the problem appears to be very hard.

References

- [1] A. Cerpa and D. Estrin, “ASCENT: Adaptive self configuring sensor network,” in *Proc. IEEE Infocom*, New York, June 2002.
- [2] A. Chandrakasan, R. Amirtharajah, S. Cho, J. Goodman, G. Konduri, J. Kulik, W. Rabiner, and A. Wang, “Design considerations for distributed microsensor systems,” in *Proc. IEEE 1999 Custom Integrated Circuits Conference (CICC)*, pp. 279–286, May 1999.
- [3] L. P. Clare, G. Pottie, and J. Agre, “Self-organizing distributed sensor networks,” in *Proc. SPIE Conf. on Unattended Ground Sensor Technologies and Applications*, pp. 229–237, April 1999.

- [4] M. Dong, K. Yung, and W. Kaiser, "Low power signal processing architectures for network microsensors," in *Proc. 1997 Int. Symp. on Low Power Electronics and Design*, pp. 173–177, August 1997.
- [5] P. Erdős and A. Renyi, "On the evolution of random graphs," *Magyar Tud. Akad. Mat. Kut. Int. Kozl.*, vol. 5, pp. 17–61, 1960.
- [6] W. Feller, *An Introduction to Probability Theory and Its Applications, Volume I*. New York: Wiley, 1965.
- [7] W. Feller, *An Introduction to Probability Theory and Its Applications, Volume II*. New York: Wiley, 1971.
- [8] P. Gupta and P. R. Kumar, "Critical power for asymptotic connectivity in wireless networks," in *Stochastic Analysis, Control, Optimization and Applications: A Volume in Honour of W. H. Fleming*, pp. 547–566, 1998.
- [9] P. Hall, *Introduction to the Theory of Coverage Processes*. New York: Wiley, 1988.
- [10] J. Karamata, "Sur un mode de croissance régulière," *Mathematica (Cluj)*, vol. 4, pp. 38–53, 1930.
- [11] V. Kawadia, S. Narayanaswamy, R. Rozovsky, R. S. Sreenivas, and P. R. Kumar, "Protocols for media access control and power control in Wireless Networks," in *Proc. 40th IEEE Conf. on Decision and Control*, Orlando, FL, December, 2001.
- [12] S. S. Kunnilyur and S. S. Venkatesh, "Network devolution and the growth of sensory lacunae in sensor networks," in *Proc. WiOpt'04: Modeling and Optimization in Mobile, Ad Hoc and Wireless Networks*, University of Cambridge, UK, March 2004.
- [13] S. S. Kunnilyur and S. S. Venkatesh, "Sensor network devolution and breakdown in survivor connectivity," in *Proc. 2004 Int. Symp. Information Theory*, Chicago, Illinois, June 27–July 2, 2004.
- [14] S. S. Kunnilyur and S. S. Venkatesh, "Network devolution and connectivity breakdown in sensor networks," preprint, 2004.
- [15] R. Meester and R. Roy, *Continuum Percolation*. Cambridge, UK: Cambridge University Press, 1996.
- [16] M. Penrose, "The longest edge of the random minimal spanning tree," *Annals Appl. Prob.*, vol. 7, pp. 340–361, 1997.
- [17] S. Shakkottai, R. Srikant, and N. Shroff, "Unreliable sensor grids: coverage, connectivity and diameter," in *Proc. IEEE INFOCOM*, San Francisco, California, 2003.
- [18] S. S. Venkatesh, "Connectivity in random geometric graphs," http://www.seas.upenn.edu/~venkates/publications_new.html, preprint, 2004.
- [19] R. Wattenhofer, L. Li, V. Bahl, and Y.M. Wang, "Distributed topology control for power efficient operation in multihop wireless ad hoc networks," in *Proc. IEEE INFOCOM*, April 2001.
- [20] F. Xue and P. R. Kumar, "The number of neighbours needed for connectivity of wireless networks," <http://decision.csl.uiuc.edu/~prkumar>, April, 2002.

DEPARTMENT OF ELECTRICAL AND SYSTEMS ENGINEERING, UNIVERSITY OF PENNSYLVANIA,
PHILADELPHIA, PA 19104
E-mail address: {kunniyur,venkatesh}@ee.upenn.edu